Building and Environment 228 (2023) 109782

Contents lists available at ScienceDirect

Building and Environment

journal homepage: www.elsevier.com/locate/buildenv

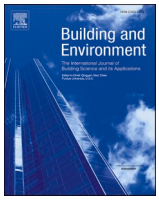

Experimental studies on electrostatic-force strengthened particulate matter filtration for built environments: Progress and perspectives

Enze Tian [a,b], Yilun Gao [c,d], Jinhan Mo [c,d,e,*]

[a] Songshan Lake Materials Laboratory, Dongguan, 523808, China
[b] Institute of Physics, Chinese Academy of Sciences, Beijing, 100190, China
[c] Department of Building Science, School of Architecture, Tsinghua University, Beijing, 100084, China
[d] Beijing Key Laboratory of Indoor Air Quality Evaluation and Control, Beijing, 100084, China
[e] Key Laboratory of Eco Planning & Green Building, Ministry of Education (Tsinghua University), Beijing, 100084, China

ARTICLE INFO

Keywords:
Indoor air quality
Electret filter
Electrospinning
PM
Ionizer
Charging

ABSTRACT

Every year, ambient particulate matter (PM) causes more than one million deaths worldwide. Considering that people spend more than 80% of their time indoors, there is an urgent need for efficient air purification in the built environment. Electrostatic forces have been armed with fibrous filters to promote filtration efficiency and avoid large pressure drops leading to large energy consumption, noise problems, and frequent replacements. Here, we summarise the electrostatic-force-strengthened filtration studies with application potentials for indoor PM removal (studies for masks, industrial processes and pollution control are not included), and divide them into three categories according to whether the PM and fibers are charged. Among them, singly-fiber-charged filtration, especially electret filters fabricated by electrospinning, serves in the simplest structure. Synergistically charging both PM and fibers outperforms the singly particle- or fiber-charged filtration, as the PM-fiber Coulombic force is far beyond the dielectrophoresis force. We introduce the working principle for each technology, compare their initial and long-term performance for non-oily particles, oily particles, and bioaerosols, and provide specific research prospects for improving the performance of these technologies.

1. Introduction

With the rapid industrialization of developing countries, expansion of global transportation, occasional wildfire and respiratory disease epidemics such as COVID-19, airborne particulate matter (PM) pollution has become an ever more important issue. Airborne PM pollution has posed serious threats not only to the performance of industrial products, but also to the population health. Responsible for various dementia, respiratory and cardiovascular diseases [1–3], airborne PM pollution has become the greatest environmental risk factor for human health, contributing to more than 0.8 million premature deaths annually [4]. The mean global urban population-weighted $PM_{2.5}$ (particulate matter with aerodynamic diameters less than 2.5 μm) concentration in 2019 was 35 $\mu g/m^3$ [5], far from the WHO air quality guideline value of 5 $\mu g/m^3$ [6]. Since people spend more than 80% of their time indoors [7], efficient PM removal devices for clean built environments have become essential.

The importance of filters for built environments has been emphasized in heating, ventilation, and air conditioning (HVAC) systems in buildings and vehicles, portable air purifiers, and clean rooms [9]. These filters can be divided into three types by their performance and treated particles (Fig. 1): (1) middle-performance filters for air intake, (2) high-performance filters for indoor air quality, and (3) high-efficiency particulate air (HEPA) filters and ultra-low penetration air (ULPA) filters for clean rooms [8]. The performance here, namely the filtration efficiency η, can be expressed by Equation (1), when an air filter is composed of same-sized cylinder fibers which are arranged perpendicular to the airflow and are packed uniformly [10]:

$$\eta = 1 - exp\left(-\frac{4\,\alpha\,L}{\pi\,(1-\alpha)d_f}\,\eta_s\right) \tag{1}$$

where α is the fiber volume fraction in the filter, L is the thickness of the filter (m), and d_f is the fiber diameter (m). The three parameters (α, L, and d_f) can be obtained from the filter geometry. The main contribution to the filtration efficiency of a single fiber, η_s, are the effects of mechanical filtration and electrostatic filtration, as shown in Fig. 2. When assuming that the mechanical filtration and electrostatic filtration are

* Corresponding author. Department of Building Science, Tsinghua University, Beijing, 100084, China.
E-mail address: mojinhan@tsinghua.edu.cn (J. Mo).

https://doi.org/10.1016/j.buildenv.2022.109782
Received 22 June 2022; Received in revised form 27 September 2022; Accepted 4 November 2022
Available online 14 November 2022

Nomenclature

d_f	fiber diameter
L	filter thickness
P	power consumption for PM and filter charging
t	testing time
v_{air}	face air velocity
W	PM holding weight amount

Greek symbols

α	fiber volume fraction in the filter
Δp	pressure drop
ε_r	relative dielectric constant
η	filtration efficiency of the filter
η_s	filtration efficiency of a single fiber
$\eta_{s,C}$	filtration efficiency of a single fiber strengthened by Coulombic force
$\eta_{s,d}$	filtration efficiency of a single fiber strengthened by dielectrophoretic force
$\eta_{s,E}$	electrostatic filtration efficiency of a single fiber
η_i	inactivation efficiency for bioaerosols
$\eta_{s,M}$	mechanical filtration efficiency of a single fiber

Abbreviations

AC	activated carbon
CA	cellulose acetate
CCD	charged coupled device
CNT	carbon nanotubes
CQF	comprehensive quality factor
DBS	dibenzylidene sorbitol
DEHS	diethyl-hexyl-sebacate
DOP	dioctyl phthalate
EAA filter	electrostatically assisted air filter
EEAF	electrostatic enhanced air filter
EEF	electrically enhanced filter
EEPF	electrostatic enhanced pleated air filter
ESP	electrostatic precipitator
FPU	fluorinated polyurethane
F–SiO_2	fluorinated alkyl modified silica
GO	graphene oxide
GPS	γ-glycidoxypropyl trimethoxysilane
HC	heterocaking
HEFS	hybrid electrostatic filtration system
HEPA filters	high-efficiency particulate air filters
HVAC	heating, ventilation, and air conditioning
IMA	ion-mediated assembly
I/O	indoor/outdoor (concentration)
MgSt	magnesium stearate
MOF	metal-organic framework
MPPS	most penetrating particle size
PA	polyamide
PAA	poly(acrylic acid)
PAN	polyacrylonitrile
PC	polycarbonate
PDA	polydopamine
PE	polyethylene
PEI	polyetherimide
PEO	polyethylene oxide
PHB	polyhydroxybutyrate
PI	polyimide
PLA	polylactic acid
PLLA	poly(L-lactic acid)
PM	particulate matter
PM_x	particulate matter with aerodynamic diameters less than x μm
PMIA	poly(m-phenylene isophthalamide)
PMMA	polymethyl methacrylate
PP	polypropylene
ppi	pores per inch
PPS	polyphenylene sulfide
PS	polystyrene
PSA	polysulfonamide
PSL	polystyrene latex
PSU	polysulfone
PTFE	polytetrafluoroethylene
PU	polyurethane
PVA	polyvinyl alcohol
PVB	polyvinyl butyral
PVC	polyvinyl chloride
PVDF	polyvinylidene fluoride
PVP	polyvinylpyrrolidone
QF	quality factor
rGO	reduced graphene oxide
SEM	scanning electron microscopy
TENG	triboelectric nanogenerator
TPP	triphenyl phosphate
TrFE	trifluoroethylene
ULPA filters	ultra-low penetration air filters
UV	ultraviolet
ZIF	zeolitic imidazolate framework

mutually independent with each other, η_s can be divided as [11]:

$$\eta_s = \eta_{s,M} + \eta_{s,E} \tag{2}$$

where $\eta_{s,M}$ and $\eta_{s,E}$ represent the single-fiber filtration efficiencies by mechanical and electrostatic force, respectively. The mechanisms of mechanical filtration for PM in built environments mainly include diffusion, impaction, and interception, and the mechanisms of electrostatic filtration include Coulombic attraction and electrophoresis. When assuming that the Coulombic and dielectrophoretic attractions are mutually independent of each other, $\eta_{s,E}$ can be divided as [11]:

$$\eta_{s,E} = \eta_{s,C} + \eta_{s,d} \tag{3}$$

where $\eta_{s,C}$ and $\eta_{s,d}$ represent the single-fiber filtration efficiencies strengthened by Coulombic and dielectrophoretic force, respectively. When both PM and the fiber are charged, the PM would be filtrated due to the combination of Coulombic and dielectrophoretic attractions. When either the PM or the fiber is charged, the PM would be filtrated due to dielectrophoretic attraction. Wang summarized the expressions for various electrostatic forces acting on a PM around a fiber [12].

Besides filtration efficiency, the pressure drop is another important performance issue when considering the performance of a filter as the large pressure drop of a high-efficiency filter can cost up to 50% of the driving fan's pressure head [14]. Since the pressure drop of a filter is positively related to the energy consumption of the driving fan, a high pressure drop means high energy cost for a filter. The pressure drop would grow even larger when the filter surface getting clogged by the captured PM [15], leading to a poor PM holding capacity that contribute to a short service life and frequent replacement of the filter [16–18].

To accomplish high-efficiency PM filtration with minimal pressure drop and maximum PM-holding capacity, applying an additional electrostatic force to fibrous filtration has been proposed as a promising method. However, the effectiveness and potential of electrostatic-force-

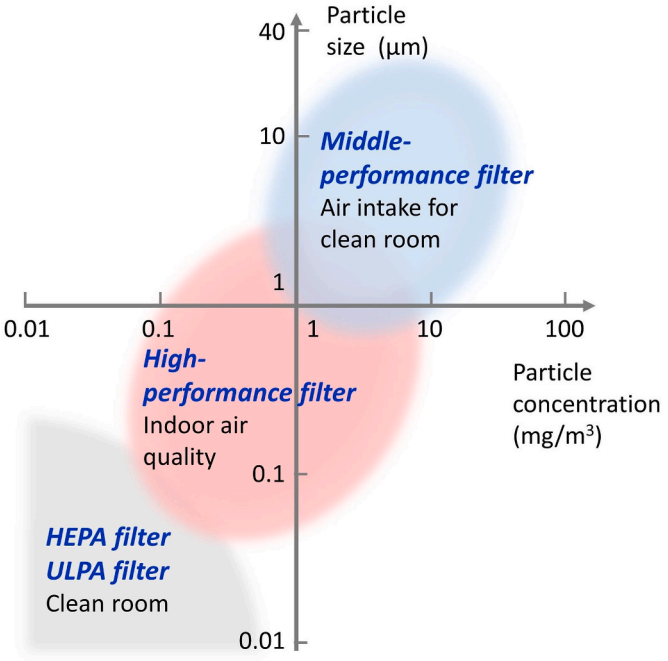

Fig. 1. Target particles for built-environment filtrations. Reproduced from Ref. [8].

strengthened filtrations for PM removal in built environments have not been systematically summarized and predicted. In this work, we focus on the experimental research progress on electrostatic-force-strengthened PM filtration studies with application potentials for indoor PM removal (studies for masks, industrial processes and pollution control are not included). To simplify the classification, we divided all electrostatic-force strengthened filtration technologies into three categories (Fig. 3): (1) singly charging the filters, (2) singly charging the PM, and (3) synergistically charging the PM and the filters. In this work, we introduce the working principle for each technology, compare their initial and long-term performance for non-oily particles, oily particles, and bioaerosols, and provide specific research prospects to improve the performance of these technologies further.

2. Strengthening electrostatic force by singly charging the filters

2.1. Electret filters

Electret filters are fibrous filters made of dielectric materials, which can carry quasi-permanent charges. They are fabricated by embedding electric charge or aligning electric dipoles within the dielectric materials [19]. The representative methods for preparing electret filters include (1) corona charging, (2) induction charging and (3) triboelectrification [20]. We summarized the performances of reviewed electret filters in Table 2.

In corona charging, dielectric fibrous materials are placed between the emitting and the receiving electrodes (Fig. 4a). The emitting electrode is often a fine wire or a point connected to a high voltage. The receiving electrode is often a plate or a cylinder connected to the ground. As a strong electric field builds up near the emitting electrode, the air around it becomes ionized. The resulting ions are driven towards the receiving electrode through the dielectric fibrous materials, on which the electrostatic charge is developed [85] (Fig. 4b). For melt-blown PP filters, Zhang et al. [21] found that the filtration efficiency was positively correlated to the glow intensity of the blue-colored corona until an electric spark appeared and destroyed the filter material (Fig. 4c and d). Thakur et al. [22,86] found that fiber diameter contributed maximum towards the filtration efficiency, followed by the grid voltage, filter basis weight, and charging voltage. Compared with conventional polymer fibers, those modified by charge enhancers (e.g., magnesium stearate [24]) show higher performance as the electret charge trapping is improved.

Induction charging, also known as electrospinning, consists of one or several nozzles applied to high voltage, and grounded surfaces for collecting the fibers. During the electrospinning, the liquid is charged and extruded from the nozzle, forms into a Taylor cone and ejects towards the grounded surfaces. The charged jet grows in a straight line and then whips because of electrical bending instability. As the jet stretches into finer diameters in the electric field, it solidifies quickly and finally deposits on the grounded collector (plate, syringe, mesh or roll-to-roll film, Fig. 5a–d) as electrospun filters [87].

The intrinsic chemical structure greatly influences electrospun filters' filtration efficiency. However, different understandings exist on whether the dipole moment (molecule level) or the dielectric constant (substance level) determines the filtration efficiency. Liu et al. [77] established that PAN had the highest filtration efficiency (>99%) among PAN, PVP, PS, and PVA due to its high dipole moment (3.6 D) (Fig. 5e and f). Cai et al. [88] indicated that PVC filter showed the highest filtration efficiency due to its highest relative dielectric constant (ε_r = 3.4), followed by the PAN, PC, and PEI filters. However, the dipole moments of PVC, PAN, PC and PEI are 1.5, 3.6, 4.1 and 0.7 D, respectively [37,89,90], drawing a different conclusion from Liu et al. [77].

A lot of nanomaterials were optimally blended to strengthen the surface potential and charge stability on electret fibers. Among them, SiO_2 is most frequently used as an ingredient to promote mechanical properties and enhance the filtration efficiency of composite filters [39,62,70,92]. By modifying SiO_2 nanoparticles with γ-glycidoxypropyl trimethoxysilane (GPS) to generate abundant stable interfacial charges, the electrospun PVDF/GPS@SiO_2 membrane exhibits a remarkable high surface potential of 12.4 kV [34]. Besides frequently used metal oxides and mineral materials, recently, some new nanomaterials including metal-organic frameworks (MOFs) [44,93], carbon nanotubes (CNTs) [49] and 2D materials [32,45,76,81,82], has been used to modify air filters due to their large surface area and great electrical properties. As for large-scale fabrication, Xu et al. [79] developed a roll-to-roll method to transfer electrospun membranes from roughed metal foil (collector) to a screen substrate, which will accelerate the commercialization of

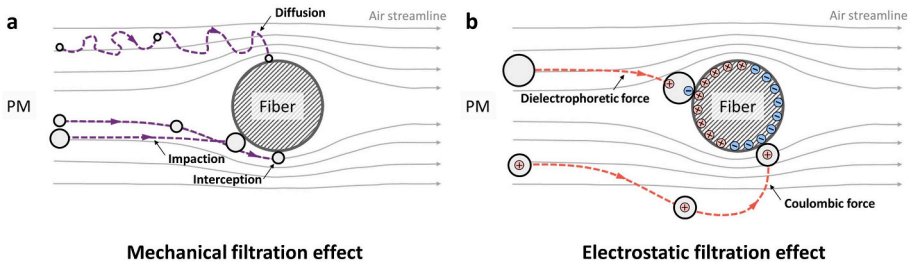

Fig. 2. Mechanism of airborne PM filtration via **a** mechanical and **b** electrostatic effects. Reproduced with permission from Ref. [13]. Copyright 2013 American Chemical Society.

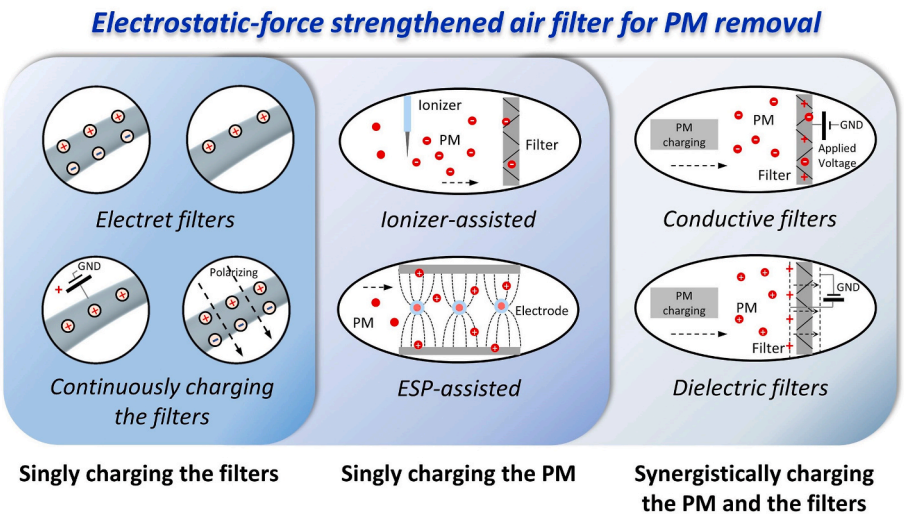

Fig. 3. Categories of electrostatic-force strengthened filtration technologies. ESP: electrostatic precipitator.

Table 1
Meaning of the base color of each box in Tables 2 and 3. The deeper blue color indicates the filter is more suitable for the clean built environment. The indicators for filtration efficiency classification are obtained according to Minimum Efficiency Reporting Value (MERV) parameters in ANSI/ASHRAE Standard 52.2–2017.

Performance grade	Filtration efficiency, η	Pressure drop, Δp (Pa)	Face air velocity, v_{air} (m/s)	Power consumption, P (W/m^2)
1	$\eta < 50\%$	$\Delta p \geq 500$	$v_{air} < 0.053$	$P \geq 100$
2	$50\% \leq \eta < 75\%$	$250 \leq \Delta p < 500$	$0.053 \leq v_{air} < 0.1$	$50 \leq P < 100$
3	$75\% \leq \eta < 85\%$	$100 \leq \Delta p < 250$	$0.1 \leq v_{air} < 0.5$	$10 \leq P < 50$
4	$85\% \leq \eta < 95\%$	$10 \leq \Delta p < 100$	$0.5 \leq v_{air} < 1$	$1 \leq P < 10$
5	$\eta \geq 95\%$	$\Delta p < 10$	$v_{air} \geq 1$	$P < 1$

transparent air filter screens. Those transparent screens can serve as windows to allow for natural ventilation and reduce the concentration of indoor $PM_{2.5}$ from outside [94].

In triboelectrification, two materials frictionally contact each other, and electrostatic charge transfers from one material to another due to their different relative electron affinities (Fig. 5g). The triboelectric process can produce interfacial charge to create an electric field, which charges the PM and removes them from the air stream [95] (Fig. 5h and i). The benefits of charging fibers by triboelectrification include: 1) it could harvest the energy from the environment for self-powered PM removal without additional power supply. 2) No hazardous ozone production during the charging process because no air discharge is needed. However, since triboelectrification occurs only at the hetero-interfaces and the produced charge can hardly penetrate thick filters, it is often used for thin membranes [84,96], applied as masks [91,97–99] and anti-haze screens (Fig. 5j) [66,84]. Although they can be self-powered by human breathing or natural ventilation, the driven energy for filter triboelectrification is from ventilation fans in building mechanical ventilation systems. Therefore, triboelectrification has not been widely studied for maintaining clean built environments. In a large-scale fabrication study, Wang et al. [83] obtained triboelectric air filters consisting of PTFE fibers modified by SiO_2 nanoparticles and PPS fibers via carding and needle-punching methods. The filtration efficiency only degraded 6.4% for a 60-day continuous operation, resulting in a powerful PM-holding capacity of 227 g/m^2.

In summary, electret filters are the most intensively studied and applied among all electrostatic-force strengthened PM filtration technologies, since they are one-time charged and do not require extra components during usage. Results in Table 2 generally indicate that the filtration efficiencies of charged filters, in descending order, are contributed by induction (electrospun fibers), triboelectrification, and corona. A PSU/TiO_2 electrospun filter showed as high as 99.997% filtration efficiency for 0.3–0.5 μm NaCl particles at 0.25 m/s air velocity, with a low pressure drop of 45.3 Pa [57]. Such high efficiency is owing to the high quantity of charge embedded into every single fiber during the fiber fabrication process of electrospinning. Due to the repulsion of spin-jets with the same charge polarity, nano-sized fibers with low pressure drop can be produced. Therefore, electrospinning, an approach to produce electrostatic-force strengthened fibers within one step, has brought prosperous research with application potential.

2.2. *Continuously charging the filters*

Though electret filters are frequently used in HVAC systems, the charge on fibers may be shielded or neutralized by the collected particles or the pass-by air moisture, thus reducing the filtration efficiency of the electret filter [100–102]. To avoid this, continuously charging the filter is considered a solution. There are typically two ways for filter charging: contact and induced, the performances of which are summarized in Table 3.

In contact charging, the conductive fibers take on charges of the same polarity as the applied power electrode and enhance their electrostatic force towards airborne PM (Fig. 6a–c). The fibers themself can be conductive [105], or they can be coated with conductive materials

[131]. The power supply of these conductive filters can be eco-friendly optimized as a triboelectric nanogenerator (TENG), which the Wang group first proposed in 2012 [132]. TENG is made from materials with excellent triboelectric properties and designed to harvest small-scale low-frequency mechanical energy from human motion and nature [133–136]. For PM removal potentially for built-environment application, Gu et al. [108] connected the electrospun PI nanofibers collected on a stainless-steel net to a rotating TENG for fiber charging, realizing filtration efficiency enhancement from 27.1% to 83.6% for 76.4 nm PM. A rotating TENG-assisted multilayer PI nanofiber filter was further developed to remove ambient ultrafine PM and microorganisms [137].

In induced charging, an external electric field is applied to filters, making filter fibers generate induced charges to create a local non-uniform field around fibers. In the meantime, the external electric field and the local electric field generated by charged fibers would also polarize the neutral particles, thereby introducing induced charges and a dielectrophoretic force on particles [13] (Fig. 6d). Li et al. [107] deposited electrospun PAN nanofibers on a metal mesh and fixed another metal mesh on it, obtaining a sandwich-structured air filter (Fig. 6e). When applying a 2 kV DC voltage through the 13 μm thick filter, the $PM_{2.5}$ filtration efficiency was enhanced from 84.41% to 98.72%. Shaping the electrodes to a "W" form, Lee et al. [104] built an external electric field of 5 kV/cm through a pleated filter in an HVAC system to investigate the effect of PM loading on filtration performance (Fig. 6f). It was found that the initial filtration efficiency (in the depth filtration process) of the filter module was increased significantly by the electric field. In contrast, the ending filtration efficiency (in the surface filtration process) showed little improvement by the electric field. Further, the pressure drop increased less as PM loading in the presence of the electric field, resulting in a large PM holding capacity of the filter module. Besides, there have been other methods (via friction [98,103,106] and magnetoelectric effect [138]) to continuously charging the filters.

In summary, continuously charging the filters enables the charge on particles and fibers to remain as long as the external power supply or electric field is on. In this way, the strengthened electrostatic force

Table 2
Performance of reviewed electret filters. The meaning of the base color of each box is illustrated in Table 1. The "~" means the value is an approximate one given by the reference article, obtained from the figures, indirect calculations or unit conversions [26,27,33,35,36,38,41,42,46–48,50–52,54,59,60,63–65,67,68,73,75,78,80].

Ref.	Filter material	PM type	PM size (μm)	η	Δp (Pa)	v_{air} (m/s)
Filter charging method: Corona						
[21]	PP	NaCl	0.26[a]	95.62%	123.2	0.141
[22]	PP	NaCl	1–3	63.49%	46	0.1
				69.97%	68	
				48.77%	38	
				57.94%	60	
[23]	PP	NaCl	0.1–2	~98.6%	22.45	0.053
[24]	PP/PE	NaCl	0.26[a]	88.27%	22.34	0.053
	PP/PE/MgSt			91.32%	22.50	
[25]	PVDF	NaCl	0.1	90%	18	0.053
				94%	26	
				93%	25	
[26]	PVDF	NaCl	0.25	~43.1%	4.3	0.053
				~65.2%	35.9	
				~50.6%	14.1	
				~67.6%	23.3	
[27]	PMMA	NaCl	0.025–0.4	86.4%	~39.1	0.1
	PEO/PS			92.2%	~31.2	
[28]	PTFE	NaCl	0.2	92%	90	0.083
[29]	-	NaCl	0.014–0.5	70%	~1.7	0.02
[30]	PLA	KCl	0.3–0.5	84%	27.2	0.053
				67%	8.5	
				88.5%	40.8	
[31]	PU/*S.flavescens*	KCl	0.02–0.6	88.4%	~7.84	0.133
Filter charging method: Induction						
[26]	PVDF	NaCl	0.25	~13.4%	4.4	0.053
[32]	PVDF	NaCl	0.3	75.79%	27.83	0.053
[33]	PVDF	NaCl	0.3	97.4%	52	0.053
				99.45%	180	

Ref.	Filter material	PM type	PM size (μm)	η	Δp (Pa)	v_{air} (m/s)
[34]	PVDF/SiO_2	NaCl	0.3	88.83%	16	0.053
			0.5	95.36%		
[35]	PVDF	NaCl	0.02–0.3	93.80%	983.9	1.26
	PVDF/graphite			98.49%	1297.7	
[36]	PVDF	NaCl	$PM_{0.3}$	69.8%	14	0.053
	PAN			64.6%	15	
	PA			59.1%	18.5	
	PU			53.1%	21.5	
[37]	PVDF/PTFE	NaCl	0.3–0.5	94.24%	18	0.053
				99.97%	57	
[38]	PVDF/negative ions powder	NaCl	$PM_{2.5}$	99.99%	80	0.053
[39]	PVDF/DBS/F-SiO_2	NaCl	0.3	99.78%	16	~0.008
			0.5	99.96%		
			0.3	99.54%	29	~0.016
			0.5	99.97%		
			0.3	98.82%	55	~0.032
			0.5	99.87%		
[40]	PAN	NaCl	0.26[a]	99.99%	126.7	0.053
[41]	PAN	NaCl	0.3–0.5	75.2%	5.2	0.053
[42]	PAN	NaCl	0.26[a]	~99.5%	~260	0.141
[43]	PS/PAN	NaCl	0.3	99.96%	54	0.053
[44]	PAN/MOF	NaCl	$PM_{0.3}$	90.2%	60.7	0.053
[45]	PAN/GO	NaCl	0.3	98.8%	55	0.053
[46]	PA/PAN	NaCl	0.3	99.99%	100	0.15
[47]	PAN/PAA	NaCl	0.3–0.5	99.99%	160	0.053
[48]	PAN/PMIA	NaCl	0.3–3	99.0%	24.52	0.05
[49]	PS/PAN/CNT	NaCl	0.3	96.37%	35	~0.013
[50]	PLA	NaCl	0.26[a]	99.87%	221.7	0.141
				99.99%	300.1	
[51]	PLA/PHB	NaCl	0.3	98.5%	160	0.053
[52]	PLLA	NaCl	0.1	99.74%	~20	0.078

Ref.	Filter material	PM type	PM size (μm)	η	Δp (Pa)	v_{air} (m/s)
[53]	PET/PLA	NaCl	0.26[a]	99.95%	198.27	0.053
				99.99%	201.11	
[54]	PS	NaCl	0.075[b]	87.0%	54	0.118
[55]	PS	NaCl	0.075[b]	86.5%	67.4	0.118
[56]	PSA	NaCl	0.3	99.8%	123	~0.056
[57]	PSU/TiO_2	NaCl	0.3–0.5	99.997%	45.3	0.25
[58]	PVB/Si_3N_4/FPU	NaCl	0.3–0.5	99.95%	55	0.053
[59]	PVC/PU	NaCl	0.3–0.5	99.5%	144	0.154
[60]	CA	NaCl	0.046	99.95%	~2450	0.45
[61]	PI/aramid	NaCl	0.4–0.5	94.83%	136	0.1
				88.86%	110	
				81.27%	76	
				70.38%	55	
[62]	PEI/SiO_2	NaCl	0.3	99.99%	61	0.053
[63]	PA	NaCl	0.3–0.5	99.32%	46	0.053
[64]	Worm silk	NaCl	0.3	96.2%	98	0.053
[65]	PAN	KCl	0.3–0.5	99.61%	282	0.05
[66]	PVDF/TrFE	KCl	$PM_{1.0}$	87.6%	63	0.35
[67]	Spider silk/PA	Arizona test dust	0.2	93%	131	0.25
[68]	Spider silk/PA	Arizona test dust	0.2	96%	198	0.492
				97%	535	0.213
	Lacewing silk/PA			69%	128	1.274
				78%	227	1.107
				78%	306	0.645
	PLA/PA			86%	193	1.091
				51%	129	1.671
	PEO/PA			22%	40	1.43
				51%	34	2.077
[64]	Worm silk	Ambient	$PM_{2.5}$	98.8%	98	0.053
[69]	Nonwoven/AC	Ambient	0.3–0.5	60%	150	~2.85
[55]	PS	DOP	0.185[b]	61.1%	67.4	0.118

Ref.	Filter material	PM type	PM size (μm)	η	Δp (Pa)	v_{air} (m/s)
[54]	PS	DOP	0.185[b]	70.1%	54	0.118
[70]	PI/SiO_2	DEHS	$PM_{0.3}$	94.38%	260	0.28
[56]	PSA	DEHS	0.3	99.7%	232	0.056
[71]	PSA/PAN	DEHS	0.3	90.93%	25	2
				99.52%	45.16	
[72]	PET	DEHS	MPPS (~0.2)	95.98%	414	0.053
	PET/silk			93.38%	272	
	Silk			39.01%	47	
[73]	PVA	PSL	0.3	96.79%	80.6	0.053
				97.38%	132.8	
	PAN			91.96%	64.6	
				95.83%	90.4	
[74]	PU	Burning cigarette	$PM_{2.5}$	98.92%	10	~0.041
[75]	Worm silk	Burning cigarette	$PM_{2.5}$	99.84%	75	0.2
[76]	PAN/$Ti_3C_2T_x$	Burning incense	$PM_{2.5}$	99.7%	42	0.053
[77]	PAN	Burning incense	$PM_{2.5}$	98.11%	206	0.21
				96.12%	133	
[78]	TPP/nylon-6	Burning incense	$PM_{2.5}$	99.06%	253	0.5
[79]	nylon-6	Burning incense	$PM_{2.5}$	99.56%	~271	0.21
[80]	PVA/cellulose	Burning incense	$PM_{2.5}$	99.1%	91.7	0.2
[81]	PAN	Burning incense	$PM_{2.5}$	95.1%	183	0.2
	PAN/GO			99.6%	117	
[82]	PAN	Burning incense	$PM_{2.5}$	95.8%	147	0.2
	PAN/GO			98.5%	112	
	PAN/GO/PI			99.5%	92	
[32]	PVDF	Burning incense	$PM_{2.5}$	93.7%	24	0.053
	GO/PVDF			99.3%	35	
Filter charging method: Triboelectrification						
[29]	-	NaCl	0.014–0.5	81%	~1.0	0.02
[83]	PTFE/PPS/SiO_2	NaCl	0.26[a]	99.7%	55.4	0.053
[66]	PVDF/TrFE	KCl	$PM_{1.0}$	94.3%	63	0.35
[84]	Nylon-6	KCl	$PM_{1.0}$	~76%	~290	0.35
			$PM_{2.5}$	~88%		
		DOP	$PM_{1.0}$	~70%		
			$PM_{2.5}$	~90%		
	Nylon-11	KCl	$PM_{1.0}$	~78%	~200	
			$PM_{2.5}$	~90%		
		DOP	$PM_{1.0}$	~48%		
			$PM_{2.5}$	~76%		

[a] mass median diameter, [b] count median diameter.

would be maintained as well as the filtration efficiency. For the initial performance, singly charging the filter shows maximum filtration efficiency of ~99.5% for $PM_{2.5}$ with a low pressure drop of ~52 Pa at 1 m/s air velocity. For more important long-term performance, we discussed them in Section 5.4.

3. Strengthening electrostatic force by singly charging the PM

Since PM in natural environments does not carry sufficient charge, the strengthened electrostatic force by singly charging the filters is not significant enough. Therefore, to achieve higher filtration efficiency or lower pressure drop, some researchers continuously charge the PM with ionizers and ESPs, the performances of which are summarized in Table 3.

3.1. Ionizer-assisted filters

Installing ionizers in front of filters is a simple method to enhance the filtration efficiency without increasing the pressure drop. A typical structure of ionizer-assisted filter is shown in Fig. 7a, where an array of carbon fiber ionizers helps PM get charged and a filter to collect PM. However, the operating environment significantly restricts the performance of ionizer-assisted filters. The device can only produce a high efficiency under low relative humidity, low particle concentration and low air velocity [139]. Using commercial filters, the largest filtration efficiency enhancement was from 5% to 73% for 0.5 μm particles at 1.1 m/s air velocity [111]. Woo et al. [140] investigated the influence of filter material on ionizer-assisted filtration using grapefruit seed extract coated PP, activated carbon fiber, and metal foam. The metal foam

Table 3
Performance of reviewed filters/filtration devices with continuously charging. The meaning of the base color of each box is illustrated in Table 1. The "~" means the value is an approximate one given by the reference article, obtained from the figures, indirect calculations or unit conversions [109,120,121].

Ref.	Filter material	PM type	PM size (μm)	η	Δp (Pa)	v_{air} (m/s)	P (W/m^2)
Singly charging the filter							
[103]	PVC/PA	NaCl	0.3	98.75%	67.5	0.1	-
[104]	PET/PP	Arizona test dust	4	98.5%	~133	2.5	-
[105]	Carbon	Ambient	$PM_{1.0}$	68.6%	2.6	0.033	-
				82.8%	4		
				89.6%	6		
				95.1%	34.2		
				95.8%	56		
				78.4%	36.8	0.067	
				72.5%	124.8	0.133	
[106]	PP/PAN/ PEDOT:PSS	Ambient	0.3–0.4	88.68%	107	0.15	-
[98]	PVDF	Burning cigarette	$PM_{0.5}$	99.4%	57	0.1	-
[107]	PAN	Burning cigarette	$PM_{2.5}$	98.72%	82	0.21	-
				93.48%	75		
				99.08%	90		
[108]	PI	Burning cigarette	$PM_{2.5}$	~97.8%	~17	1	-
				~99.5%	~52		
Singly charging the PM							
[109]	Glass	KCl	0.1	~23%	~226	0.4	< 625
				46.9%	~284	0.5	
				~18%	~343	0.6	
				~12%	~461	0.8	
[110]	PP/Glass	DOP	0.4–2.5	~100%	38	0.1	~15.2
[111]	PE	PSL	0.5	~73.4%	82	1.1	-
				~17.7%	68		
			1	~86.0%	82		
				~58.7%	68		
Charged conductive filters with PM precharged							
[112]	PE/Al	KCl	0.03–0.4	~99.99%	~4.9	0.1	-
[113]	PET/Al	KCl	0.03–0.41	~98.4%	0.8	0.05	-

Ref.	Filter material	PM type	PM size (μm)	η	Δp (Pa)	v_{air} (m/s)	P (W/m^2)
[114]	ZIF-8/Cu/PAN	Cu	<1.5	94.0%	69	0.425	-
				97.9%	207		
[115]	Ni	Ambient	0.3–0.5	78.9%	10.8	0.5	18.7
[116]	Stainless steel	PSL	1	~95%	-	1	~226
[117]	Stainless steel	PS	0.05–1	98%	~237	0.3	~161
				97%	~199		
				96%	~87		
[117]	Stainless steel	PS	0.05–1	97%	~648	0.75	~161
[118]	Ag/nylon	Burning incense	$PM_{2.5}$	99.99%	10.34	0.11	-
[119]	Ag/nylon	Burning sandalwood	$PM_{2.5}$	99.48%	14.43	0.2	-
Charged dielectric filters with PM precharged							
[120]	PP	NaCl	0.1	98.20%	~113[a]	0.053	-
	PA			99.30%	~428[a]		
[121]	PP	NaCl	0.07	99.8%	<2	0.0068	~7.64
[122]	PDA/PET	KCl	0.3–0.5	99.48%	9.5	0.4	~22.4
				96.74%	29.5	1.0	
				90.72%	75.7	2.0	
				76.91%	215	3.7	
	PET			89.66%	9.0	0.4	
				80.81%	34.5	1.1	
				75.24%	84.9	2.1	
				56.71%	220	3.8	
	PVDF/PET			92.98%	10.8	0.4	
[123]	PP/glass	Arizona test dust	0.4	97%	38	0.1	~8.75
[124]	-	Arizona test dust	7.6[b]	92.9%	~118	2.5	0.38
[125]	PU	Ambient	0.011–0.115	78.28%	10.4	1	10.2
			0.3–0.5	71.00%			
	PU/AC		0.011–0.115	90.47%	12.3		
			0.3–0.5	85.52%			
	PU/MnO_2		0.011–0.115	90.50%	13		

Ref.	Filter material	PM type	PM size (μm)	η	Δp (Pa)	v_{air} (m/s)	P (W/m^2)
			0.3–0.5	85.38%			
[126]	PU	Ambient	0.3–0.5	54.7%	3.5	1.1	67.0
	PU/MnO_2			84.2%	4.2	1.1	71.0
	PU/AC			84.9%	3.6	1.1	69.9
	PU/AC			78.4%	4.1	1.1	32.0
	PU/ZnO			87.0%	3.8	1.1	71.1
	PU/CuO			84.6%	3.5	1.1	70.3
[127]	PE	Ambient	0.3–0.5	69%	66	0.5	~3.56
[128]	PET	Ambient	0.3–0.5	99.0%	21.0	1.2	59.2
				74.7%	11.6	1.1	16.0
				95.5%	16.6	1.2	19.0
				93.2%	12.0	1.1	18.3
[129]	PET	Ambient	0.3–0.5	94.4%	5.9	1	5.9
				90.3%	14.7	2	5.9
				85.0%	26.4	3	6
[130]	$CA/AC/TiO_2$	Ambient	0.3–0.5	82.29%	63.8	0.8	35.7
[69]	Nonwoven/AC	Ambient	0.3–0.5	95%	150	~2.85	8.03

[a] calculated by Davies empirical correlation [10], [b] mass median diameter.

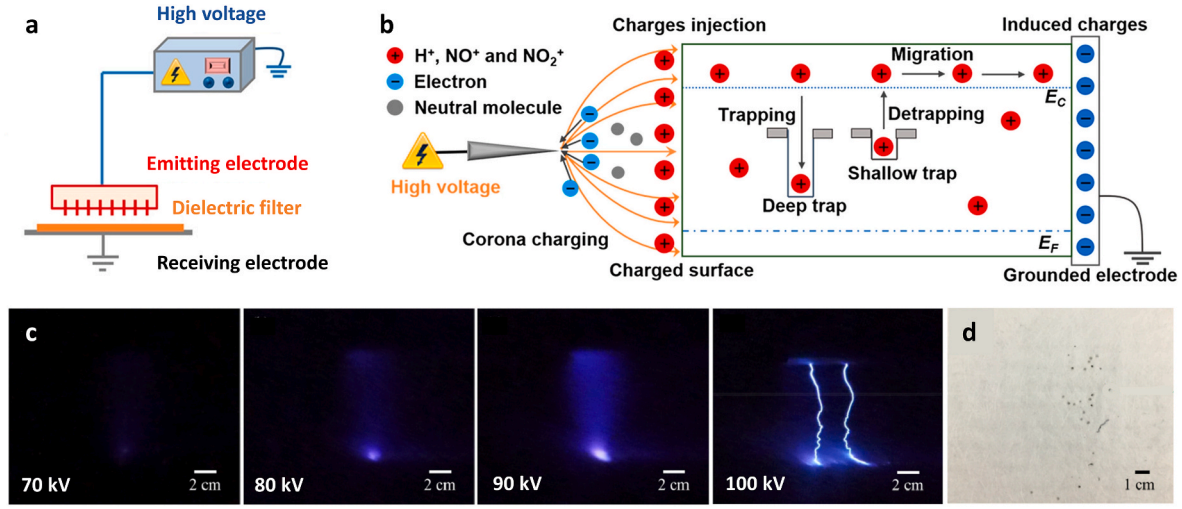

Fig. 4. Illustration for corona charged electret filters. **a** The prototype and **b** the mechanism of corona charging for electret filters [24]. Reproduced with permission from Ref. [24]. Copyright 2019 American Chemical Society. **c** Blue-colored glow phenomenon at 70–100 kV corona charging voltages [21]. **d** The photograph of the filter destroyed by an electric spark [21]. Reproduced with permission from Ref. [21]. Copyright 2018 Wiley-VCH. (For interpretation of the references to color in this figure legend, the reader is referred to the Web version of this article.)

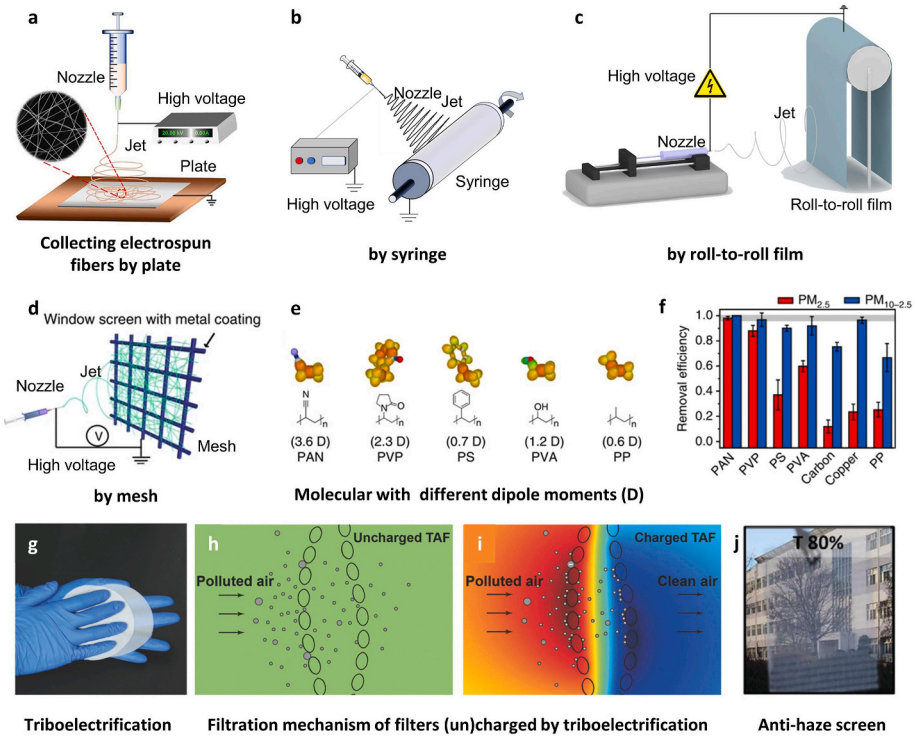

Fig. 5. Illustration for electret filters charged by electrospinning and triboelectrification. The schematics of electrospinning using **a** plate [81], (Reproduced with permission from Ref. [81]. Copyright 2019 American Chemical Society) **b** syringe [25], (Reproduced with permission from Ref. [25]. Copyright 2020 Elsevier) **c** roll-to-roll film [74], (Reproduced with permission from Ref. [74]. Copyright 2019 IOP Publishing) and **d** mesh [77] as collecting electrodes. **e** Molecular model, formula, calculated dipole moments and **f** PM removal efficiency of different materials [77]. Reproduced with permission from Ref. [77]. Copyright 2015 Springer Nature. The schematics for **g** triboelectrification process and filtration mechanism of **h** uncharged and **i** charged filter [91]. Reproduced with permission from Ref. [91]. Copyright 2018 Wiley-VCH. **j** Photographs of anti-haze screen charged by triboelectrification with 80% transparency [66]. Reproduced with permission from Ref. [66]. Copyright 2019 Wiley-VCH.

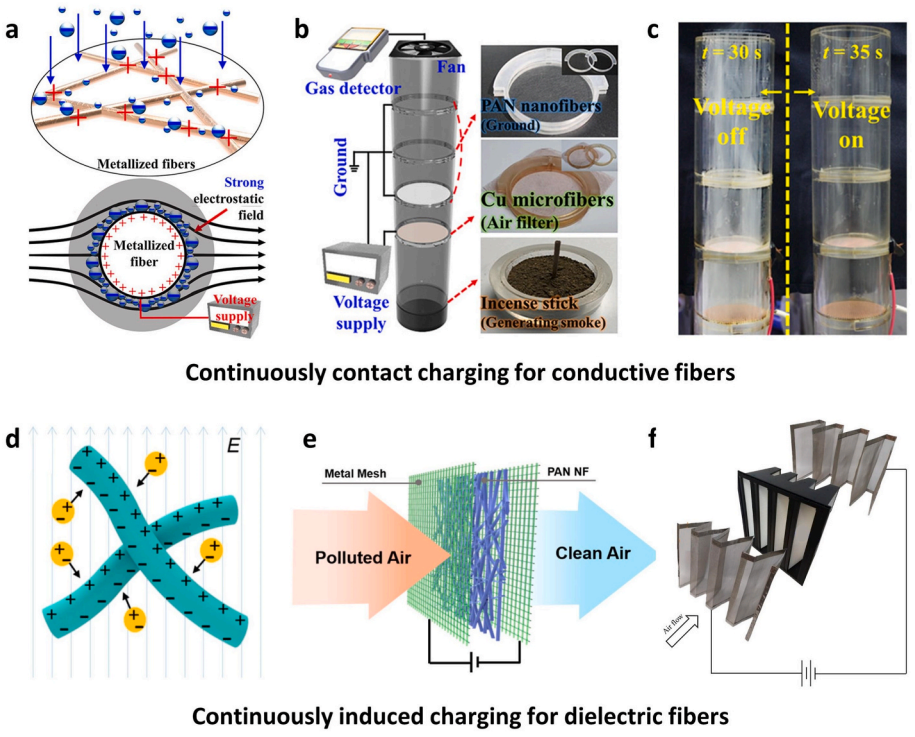

Fig. 6. Strengthening electrostatic force between the filter and the PM by continuously charging the filter. **a** The schematic, **b** experimental setup, and **c** photographs of PM filtration by charging metalized fibers [131] (Reproduced with permission from Ref. [131]. Copyright 2019 American Chemical Society). **d** the filtration mechanism and **e** the prototype of the filter continuously charged by induction [107] (Reproduced with permission from Ref. [107]. Copyright 2018 American Chemical Society). **f** the W-shaped module for filter induced charging [104] (Reproduced with permission from Ref. [104]. Copyright 2020 Elsevier).

showed the lowest pressure drop (<80 Pa at 0.05 m/s air velocity) and an increase in collection efficiencies for *S. aureus* aerosol (0.7 μm) from 72% to 98% after turning on the ionizer [69].

3.2. ESP-assisted filters

Another widely used PM charging method is via electrostatic precipitators (ESPs) [142,143]. The ESPs accomplish corona charging in the air using a high-voltage electrode with a small curvature radius, including wires and points. The airborne PM gets charged with the same polarity as the high-voltage electrode when it collides with the charged air molecules. The charged PM aggregates towards and deposits on an oppositely charged (or grounded) collecting electrode (Fig. 7b) [141]. Limited by the length and superficial area of collecting electrodes, the

ESP has low filtration efficiency for fine particles [142] and small PM holding capacity [144]. Therefore, the combination of ESP and fibrous filters has been proposed as a promising way to achieve persistent high-efficiency and large PM holding capacity. In fact, in many industrial cases, adding a filter to the exhaust of an ESP is a conventional technology named hybrid electrostatic filtration [145–149].

For built-environment application, Feng et al. [110] systematically investigated the influence of factors (such as filter types, ESP applied voltage, and the distance between the ESP and the filter) on the filtration efficiency and ozone production of a hybrid electrostatic filtration system (HEFS) (Fig. 7c). It was found that the HEFS's performance was sensitive to filter type and applied voltage (Fig. 7d and e). Positive discharge produced less current and ozone than a negative one, although it also led to slightly less filtration efficiency. An optimal HEFS supplied with +8 kV produced ~40 ppb ozone at 1 m/s air duct velocity, while a single ESP supplied with +12 kV produced ~300 ppb ozone [110]. The HEFS was further examined for its SARS-CoV-2 aerosol removal performance. Among UV + Filter, fibrous filter, HEFS and ESP, UV + Filter was the most reliable and safest technology, although it consumed the highest energy, followed by fibrous filters, HEFA and ESP [150]. The biggest obstacle to the ESP-assisted filter should be the by-product of ozone. Xiang et al. [151] and Day et al. [152] examined the performance of the combined use of an ESP and a HEPA filter in building ventilation systems and investigated its effects on cardiorespiratory health. When the supply air ozone level was above 18 ppb, the average indoor PM level would increase by 22000 pcs/cm^3 [151].

4. Strengthening electrostatic force by charging both the filters and the PM

When either particles or filters are charged, the electrostatic force between them is relatively weak and the enhancement of electrostatic filtration efficiencies is insufficient. Therefore, simultaneous charging of particles and fibers seems to be a good solution to obtain higher filtration efficiency or lower pressure drop. Particles are usually precharged by ionizers or corona discharge, while the filters are usually charged by contact or polarization.

4.1. Charged conductive filters with PM precharged

Charging PM and conductive filters are like transforming ESP's collecting electrodes from plates to conductive filters [153]. The transformation makes charged particles go through rather than in parallel to the collecting electrodes, showing a higher probability of particle removal from air flow. Mermelstein et al. [117] optimized structure and pore size of stainless-steel filters to realize the best filtration efficiency of 92% for 0.05–1 μm particles, while the pressure drop was around 299 Pa at 0.75 m/s air velocity. To reduce the pressure drop, Tian et al. [115] used metal (Ni, FeNi, Fe and Cu) foams as the collecting electrodes (Fig. 8a). Optimized by a proposed structural coefficient $N_{s,E}$, a 75-ppi Ni foam can remove 0.3–0.5 μm particles with an efficiency of 78.9% and a low pressure drop of 10.8 Pa at 0.5 m/s air velocity (Fig. 8b). Jung et al. [154] introduced reduced graphene oxide (rGO) to Cu mesh by ion-mediated assembly (IMA) and thermal reduction (Fig. 8d). With the assistance of an ionizer, the charged filter resulted in >99% filtration efficiency for $PM_{2.5}$ after 5 cycles of cleaning and reuse (Fig. 8c,e).

Besides metal filters, some researchers also coated polymer filters with metal to fabricate conductive filters [112–114,118,119,155,156]. With the assistance of an ionizer (Fig. 8f), the Al-coated filters showed a 99.99% filtration efficiency for 0.03–0.4 μm particles, due to the strong electrostatic force between the charged fibers and particles (Fig. 8g) [113]. The Al-coated conductive fibrous filters with reinforced hydrophobicity and surface roughness also showed antimicrobial activity against airborne *E. coli* and *S. epidermidis* with efficiencies of ~94.8% and ~96.9%, respectively (Fig. 8h) [155]. For large-scale fabrication, Huang et al. [119] prepared a 7.5 m^2 Ag nanowire nylon air filter in 20 min via one-step ink coating, realizing 99.48% filtration efficiency for $PM_{2.5}$ with a pressure drop of 14.43 Pa at 0.2 m/s air velocity.

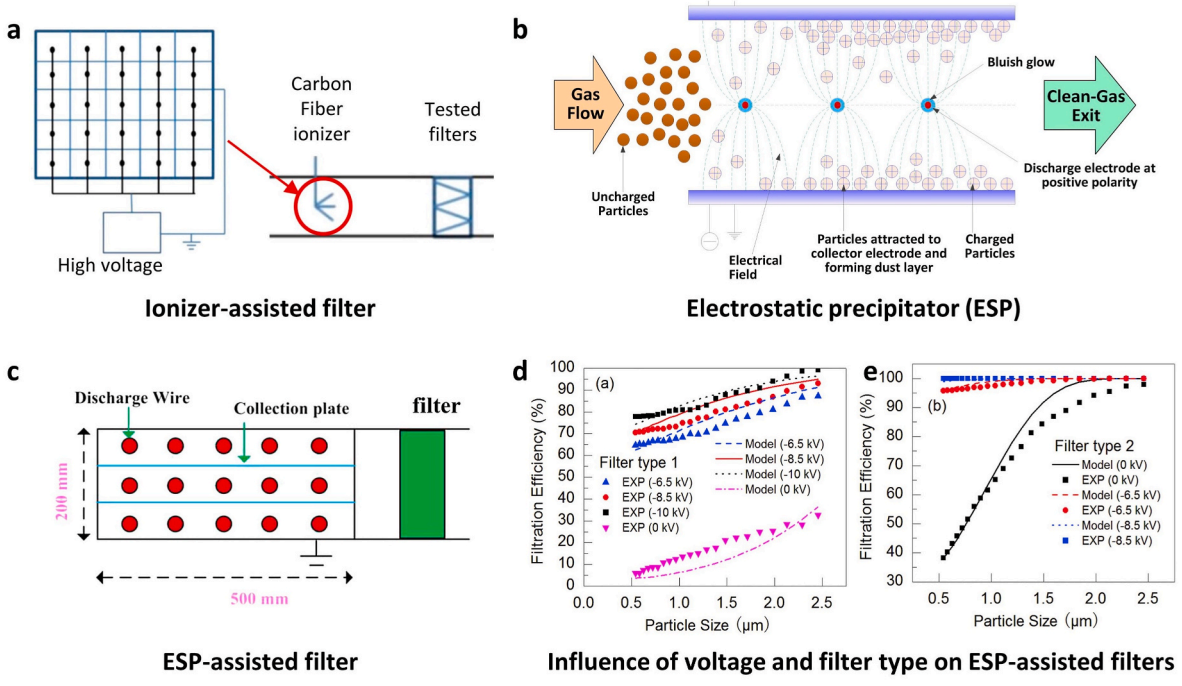

Fig. 7. Strengthening electrostatic force between the filter and the PM by singly charging the PM. The schematics for **a** an ionizer-assisted filter [139] (Reproduced with permission from Ref. [139]. Copyright 2015 American Chemical Society) **b** an ESP [141] and **c** an ESP-assisted filter [110]. Comparison of the modelled and measured filter efficiencies with different ESP charging voltages using **d** type 1 filter and **e** type 2 filter downstream [110]. Reproduced with permission from Ref. [110]. Copyright 2016 Elsevier.

4.2. Charged dielectric filters with PM precharged

For conductive filters, most charged particles were captured by Coulombic interactions via surface filtration [113]. The electrostatic shielding limits these filters' filtration efficiency and PM holding capacity because there is no electric force inside the conductive filter. Therefore, synergistic charging particles and dielectric (nonconductive) filters were proposed as an inspiring way to achieve high efficiency, low pressure drop, and large PM holding capacity simultaneously.

Dielectric filters can be one-time charged as electret filters [69,130,157] (Fig. 9a). Kulmala et al. [69] installed a separate particle charging section upstream of electret filters in a building HVAC system. They found that the additional PM charging increased the filtration efficiency for 0.3–0.5 μm PM from 60% to 95%, resulting in the I/O ratio decreasing from 0.67 to 0.40. As the charge in electret filters may decay with time, continuously charging to dielectric filters by polarizing is considered a solution. Feng et al. [123] proposed an electrostatic enhanced air filter (EEAF) system which had a pin-filter medium--grounded conductive plate structure (Fig. 9b, left). The pin connected to the high voltage would generate corona discharge where particles get charged. At the same time, an uneven electric field was generated between the charged pin and the grounded plate, penetrating and polarizing the filter medium. The filtration efficiency for 0.4 μm particles was enhanced to 97% with an applied voltage of 25 kV and a pin-filter distance of 100 cm at a face air velocity of 0.1 m/s. Feng et al. [158] further transformed the flat filter into a pleated filter (Fig. 9b, right), improving the filtration efficiency (20%) and saving energy consumption (75%). However, as both particles and the filter medium were charged in the electric field between high voltage and grounded electrodes, it was difficult to optimize the filtration performance by adjusting particle and filter charging separately.

Lee et al. [124] separated the charging fields for particles and the filter by using a two-stage electrostatically augmented air filter, which consisted of an ESP precharger and an electrified filter collector. In the ESP precharger, particles got charged by positive corona in a 4.7 kV/cm electrical field. In the electrified filter collector, a folded filter was polarized by meshy metal separators in a 1.4 kV/cm electrical field. The filtration efficiency for 0.1–5 μm particles rose from 70.0% (without electric field) to 92.9% with the two-stage charging. This device had a relatively large and complex structure with a pressure drop of 12 mmAq (~118 Pa) at 2.5 m/s face air velocity. To make the structure more compact, Lachendro et al. [159] proposed an electrically enhanced filter (EEF), which incorporated a particle pre-charging electrode and a fibrous filter in an electric field. The EEF showed significant inactivation of all vegetative bacterial cells in 4 h but did not mention the particle filtration efficiency and pressure drop.

Approaching the minimal pressure drop, Tian et al. [127] proposed a compact electrostatically assisted air (EAA) filtration module based on coarse filters. The strong and uneven electric field between the high-voltage wires and the grounded front screen caused corona discharge and charged the particles (Fig. 9c). The relatively weak electric field between the high-voltage wires and the grounded back screen polarized the filter fibers with untransferable charges on their surfaces. At an optimal charging voltage (+9 kV) and polarizing distance (4.5 cm), the filtration efficiency of the compact EAA coarse filter for 0.3 μm particles increased from 4% to 69% with a constant pressure drop of 66 Pa at 0.5 m/s. Though the efficiency was not satisfyingly high, it was found that filter materials of larger ε_r or larger tortuosity yielded higher filtration efficiencies. To realize a higher filtration efficiency, Tian and Mo developed a new EAA filter, in which particle precharging and filter

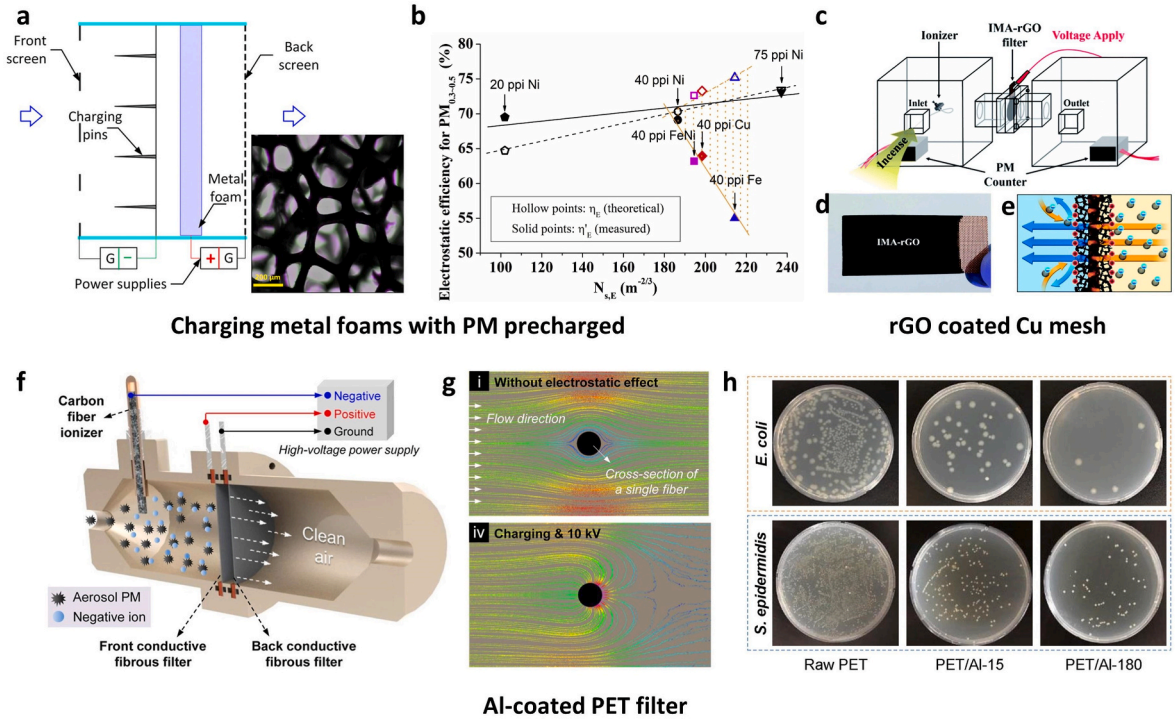

Fig. 8. Strengthening the electrostatic force between the filter and the PM by charging conductive filters with PM precharged. The schematics for collecting charged PM by **a** a metal foam [115] (Reproduced with permission from Ref. [115]. Copyright 2018 Elsevier), **c, e** a rGO coated Cu mesh filter [154] (Reproduced with permission from Ref. [154]. Copyright 2018 Royal Society of Chemistry), and **f** two Al-coated PET fibrous filters [112]. **b** The relationship between the structural coefficient ($N_{S,E}$) and the theoretical and measured electrostatic filtration efficiencies of the metal foam [115]. Reproduced with permission from Ref. [115]. Copyright 2018 Elsevier. Photographs of **d** rGO coated Cu mesh filter [154] (Reproduced with permission from Ref. [154]. Copyright 2018 Royal Society of Chemistry), **h** recultivated *E. coli* and *S. epidermidis* colonies from raw and Al coated PET [155] (Reproduced with permission from Ref. [155]. Copyright 2018 Elsevier). **g** Trajectories of neutral particles near an uncharged Al coated PET fiber (upper) and charged particles near a 10 kV charged Al coated PET fiber (down) [112].

polarizing fields were independently controlled and optimized [128]. The device remarkably increased the filtration efficiency of a coarse filter from 0.4% to 99.0% with a 21.0 Pa pressure drop at 1.2 m/s filtration velocity.

Subsequently, our group optimized and improved the EAA filtration module from particle precharging and filter polarizing aspects. Gu et al. [160] added a particle-free protection air circuit to the pin-to-plate discharger to prevent it from being polluted (Fig. 9e). The protected pins produced less ozone and had higher breakdown voltage than the unprotected pins, thus having better long-term performances. Mo et al. [129] pleated the polarizing electrodes and the filter between them to 45°, achieving high filtration efficiency for 0.3–0.5 μm particles (85.0–94.0%) and low pressure drop (5.9–26.4 Pa) at high air duct velocity (1–3 m/s). Tian et al. [126] optimized the filter material by fabricating heterocaking (HC) filters with ultralow pressure drop (3.5–4.2 Pa at 1 m/s face air velocity). High-ε_r inorganic HCs, including MnO_2, AC, ZnO, CuO and $BaTiO_3$, were loaded on PU foams by adhesive. Observing via a CCD camera, Tian et al. revealed charged particles' migration speed and trajectory towards a single polarized HC fiber (Fig. 9f and g). With catalyst and adsorbent loaded, the filters can remove not only particles but also ozone [125,126], formaldehyde [126] and phthalic acid esters [161]. However, to avoid adhesive blocking airways, this method required substrate filters of large pores, which allow some particles to bypass the collecting media. The highest filtration efficiency of the EAA HC filter for 0.3–0.5 μm particles was less than 90%. To add electrostatic responsive material to bulk fibrous filter thoroughly and firmly, Tian et al. [122] proposed to coat PET coarse filter with polydopamine (PDA) (Fig. 9h and i) by an *in situ* dopamine polymerization process. By modifying the surface ε_r and microstructure of fibers with an optimized amount of precursor, the PDA-coated PET filter reached the highest filtration efficiency (99.48% for 0.3 μm particles) with a maintained low pressure drop of 9.5 Pa at 0.4 m/s. The device design principles and materials selection criteria were delineated, giving a complete-process theoretical framework for this type of device (Fig. 9d).

5. Performance for PM removal in built environments

Key parameters for evaluating filters strengthened by the electrostatic force include single-pass filtration efficiency (η), pressure drop (Δp), power consumption (P), quality factor (QF), and comprehensive quality factor (CQF) [162]. At the same air velocity (v_{air}), a filter/-filtration module with higher η with lower Δp and P contributed to a higher QF and CQF, indicating a cost-efficient filter/filtration module.

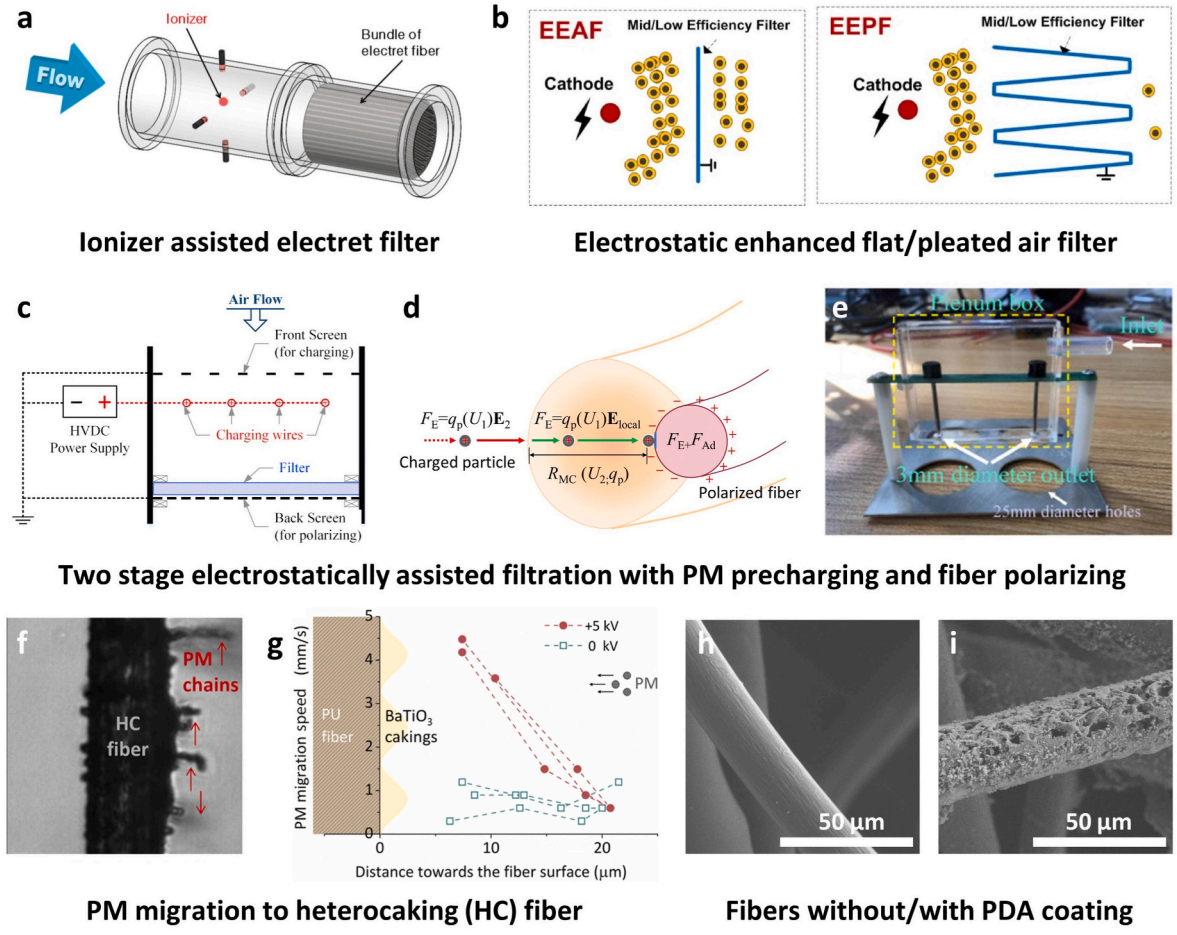

Fig. 9. Strengthening the electrostatic force between the filter and the PM by charging dielectric filters with PM precharged. The schematics for collecting charged PM by **a** a bundle of electret fiber [157] **b** polarized flat filter (EEAF) and polarized pleated filter (EEPF) [158] (Reproduced with permission from Ref. [158]. Copyright 2019 Elsevier). The schematics for **c** the compact electrostatically assisted air (cEAA) coarse filter [127] (Reproduced with permission from Ref. [127]. Copyright 2018 Elsevier) and **d** the interactions between a charged particle and an *in situ* polarized fiber in three regions [122]. (Reproduced with permission from Ref. [122]. Copyright 2021 Wiley-VCH). Photographs of **e** the particle-free protection air circuit for the pin-to-plate discharger [160], and **f** smoke particles depositing on the heterocaking (HC) fiber when +5 kV was applied [126]. **g** The PM migration speed towards the HC fiber at different positions [126]. Reproduced with permission from Ref. [126]. Copyright 2020 American Chemical Society. The SEM images of the **h** bare and **i** the PDA coated fibers [122]. Reproduced with permission from Ref. [122]. Copyright 2021 Wiley-VCH.

5.1. Non-oily PM removal

Researchers usually use inorganic salt (NaCl and KCl) and natural particles (Arizona test dust and ambient particles) to examine filter filtration efficiency for non-oily PM. These PMs are usually polar and easily get charged. For electret filters, uncharged particles would deposit all around the fibers' surface, forming chain-like agglomerates in relatively irregular patterns as the electrostatic force weakens when particle-fiber distance increases (Fig. 10a). Charged particles formed chain-like agglomerated in a more concentrated area along the electric force line (Fig. 10b) [163].

As shown in Tables 2 and 3, simultaneous high filtration efficiency and low pressure drop can hardly achieve at large air velocity. As filtration performance is only comparable when filters/devices are tested at close air face velocity and for PM with similar size [164], we consider two conditions with plenty of results: at (1) ~0.053 m/s (Fig. 10e) and (2) 1–1.2 m/s air velocity (Fig. 10f and g) for PM with a diameter in the range of 0.2–0.5 μm. It seems electret filters charged by electrospinning show the best performance among all electret filters owing to their low pressure drop when achieving high filtration efficiency. One reason for this may be that the extensive research in electrospinning has advanced the electrospun fibers' properties. Another reason may be the electrospun fibers' intrinsic electrostatic and structural properties. Gao et al. [165] compared the electret mechanisms, charge degradation kinetics and filtration lifetime of corona-charged and electrospun filters by exposing them to isopropanol vapor and high-humidity air. It was found that electrospun filters have a longer charge retention time compared to corona-charged filters and form volume charges in traps with deep energy levels during electrospinning. When comparing the corona and triboelectrically charged electret filters, Kerner et al. [29] found that the filters charged by different methods showed similar deposition characteristics when loading particles in a bipolar equilibrium charge state. However, different charge distributions led to significant differences in the fractional deposition efficiency up to 15%, even if the amount of charge and the area ratio of positive and negative charges were the same. Prawatya et al. [166] drew a different conclusion that the electric potential at the surface of triboelectrically charged polymers is less uniform, but decays slower than that of corona charged samples. More studies are needed to confirm the optimal charging methods for various electret fibrous filters and achieve stable and efficient PM filtration. Besides, structural characteristics including fiber diameter, filter thickness, and packing density [164], fiber/pore size distribution [40,43], and fiber orientation [53] could also significantly influence filtration performance.

When challenged with high air velocity, however, electrospun electret filters would show high pressure drop (~200 Pa at ~1.1 m/s air velocity) due to their small gaps (~1 μm, Fig. 10c) between fibers for airflow path. By contrast, EAA filters using coarse filters with large fiber gaps (~200 μm, Fig. 10d) demonstrated one to two orders of magnitude lower pressure drop than electrospun filters with similar filtration efficiency. It is because both particles and filters will be electrified in EAA filtration, and the Coulombic force between them will surpass dielectrophoresis force, which is the dominating interaction between neutral particles and electrospun filters. Gao et al. [125] calculated and proved that in a single-fiber model, the PM-fiber Coulombic force is $10^5 \times$ larger than the dielectrophoresis force. A most overlooked issue for EAA filters and other electrostatic filtration devices is the additional power they consume for the PM and filter charging. To avoid this, we used CQF to fairly compare the overall performance of electrospun and EAA filters. The only difference between QF and CQF is that CQF assumes the extra power consumption of charging particles and filters for efficiency improving as the equivalent resistance of the filter [115]. As shown in Fig. 10g, EAA filters still achieved a higher CQF than electrospun filters when filtration efficiency, pressure drop and energy consumption for charging were all considered. Therefore, EAA filters offer a practical trail for high-air-velocity (>1 m/s) ventilating systems for a safe, healthy, energy-saving built environment. More studies on air filtration technologies strengthened by electrostatic force are encouraged for high-air-velocity filtration for wider applications.

5.2. Oily PM removal

Researchers usually use organic and smoke particles to examine filter filtration efficiency for oily PM. These PMs are usually nonpolar and harder than non-oily PMs to get charged. The fibers would capture the solid-phase oily PM in a similar way that non-oily PM is being captured. However, some liquid-phased oily PM (droplet) would behave differently. The wetting droplets with small contact angles would move, agglomerate, and form axisymmetric conformations on fibers (Fig.11a and c). On the contrary, the non-wetting droplets with large contact angles would form a non-axisymmetric conformation (Fig. 11b and d) [167]. Therefore, electrostatic force strengthened filtration for oily PM removal usually showed a lower filtration efficiency and a higher pressure drop than for non-oily PM removal [56].

As shown in Tables 2 and 3, when considering filtration performance tested at close air face velocity and for PM with a similar size, we consider results tested at ~0.2 m/s for $PM_{2.5}$ (Fig. 11e). It seems the conductive filter assisted with an ionizer show the best performance among the selected results owing to their low pressure drop when achieving high filtration efficiency. Despite this, most literature did not mention the filtration device's additional power consumption to charge the PM and the fibers. In the limited studies that gave energy consumption results, singly charging the PM by an ESP consumed less energy (15.2 W/m^2 [110]), but simultaneously charging the particles by a corona discharge and charging the conductive fibers by contact consumed more energy (~161 [117] to ~226 W/m^2 [116]).

Not only energy consumption but also filtration efficiencies for smaller particles should be more considered. For example, an ionizer-assisted PE filter showed ~86.0% filtration efficiency for 1 μm PSL particles, but the efficiency decreased to ~73.4% for 0.5 μm particles [111]. Smaller particles, including ultrafine PM with an aerodynamic diameter of less than 0.1 μm, account for more than 73% of ambient PM in quantity [168]. Due to their larger surface area and smaller size, submicron and ultrafine PM can easily enter deeper into the body and pose a more serious health risk [169]. Therefore, more studies are encouraged to improve the filtration efficiency for smaller particles in the future.

5.3. Bioaerosol removal and inactivation

Recently, the outbreak of various infectious diseases has led to an increasing concern about bioaerosol removal and inactivation. *Escherichia coli* (*E. coli*), *Staphylococcus aureus* (*S. aureus*), and *Staphylococcus epidermidis* (*S. epidermidis*) are mostly used to examine filter removal and inactivation efficiency for bacteria. These bioaerosols are usually larger than inorganic and manufactured particles (>0.7 μm), and therefore are more easily removed by filtration. As shown in Table 4, the filtration efficiencies of electrostatic force strengthened filters were over 93.3% for bioaerosols. However, the purification of bioaerosols should go beyond filtration. For the more important process of inactivation, the efficiencies for different bioaerosols are quite different. For example, when charged by corona, nearly all bacteria (*Bacillus subtilis*, *Mycobacterium parafortuitum*, and *Pseudomonas aeruginosa*) died after being captured by the polarized filter, but the spores of *Bacillus subtilis* all survived [159].

In addition to bacteria, viruses have smaller sizes (~100 nm) and their removal and inactivation are becoming increasingly important. For example, SARS-CoV-2, having the ~80-nm-diameter lumen [170], has been confirmed to transport through aerosols and droplets produced by humans [171]. Though UV light, heating, and chemical sterilizers have been proven to inactivate viruses [172–174], there are few experimental results for filtering viruses due to limited access to high-level biosafety

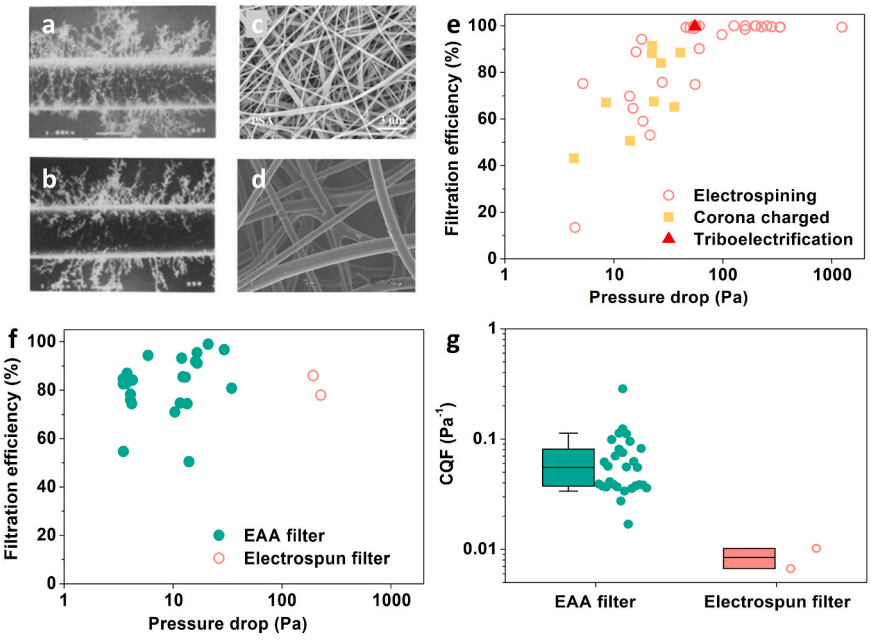

Fig. 10. Accumulations of **a**n uncharged and **b** charged PM on a single electret fiber [163]. Reproduced with permission from Ref. [163]. Copyright 2001 Elsevier. SEM images of **c** electrospun nanofibers [71] (Reproduced with permission from Ref. [71]. Copyright 2019 American Chemical Society) and **d** microfibers in coarse filters [128] (Reproduced with permission from Ref. [128]. Copyright 2019 Elsevier). Filtration efficiency for PM with a diameter in the range of 0.2–0.5 μm and pressure drop of **e** electret filters tested at ~0.053 m/s air velocity and **f** filters tested at 1–1.2 m/s air velocity. **g** Comprehensive quality factor (CQF) for PM with a diameter in the range of 0.2–0.5 μm for filters tested at 1–1.2 m/s. The data in **e**–**g** were selected from Tables 2 and 3.

laboratories. In the future, experimental studies are encouraged to verify the effectiveness of electrostatic-force strengthened filtration against various respiratory infectious viruses.

5.4. Long-term performance

Filtration efficiency degradation is a crucial problem, which limits the application of PM filtration strengthened by electrostatic force. To prompt into practice, it is important to provide the lifelong performance (Table 5) and influencing factors.

For electret filters, the charges on fibers dissipate over time, so their efficiency decreases during the operating time. For example, the filtration efficiency of an electrospun PVDF/PTFE filter decreased from 94.24% to ~83.3% only after 5 h [37]. Even without operating, a 7-day storage can degrade the filtration efficiency of electret PLA fabrics from 88.5% to ~81%, and the efficiency can drop to ~67% after a 200-day storage [30]. The influencing factors for charge and filtration efficiency degradation lie in the conductivity of loading particles [28], charging method [165], air temperature and humidity [23,177]. Electret filters may increase filtration efficiency, but at the expense of steeply increased pressure drop when they get clogged by the loaded PM. For example, a 5-min NaCl PM loading increased the filtration efficiency of a PI/aramid filter from 94.83% to ~99.8%, but also increased the pressure drop from 136 to ~400 Pa [61].

PM holding weight amount (W) is more practically meaningful than testing time (t) when considering the service life of a filter. As shown in

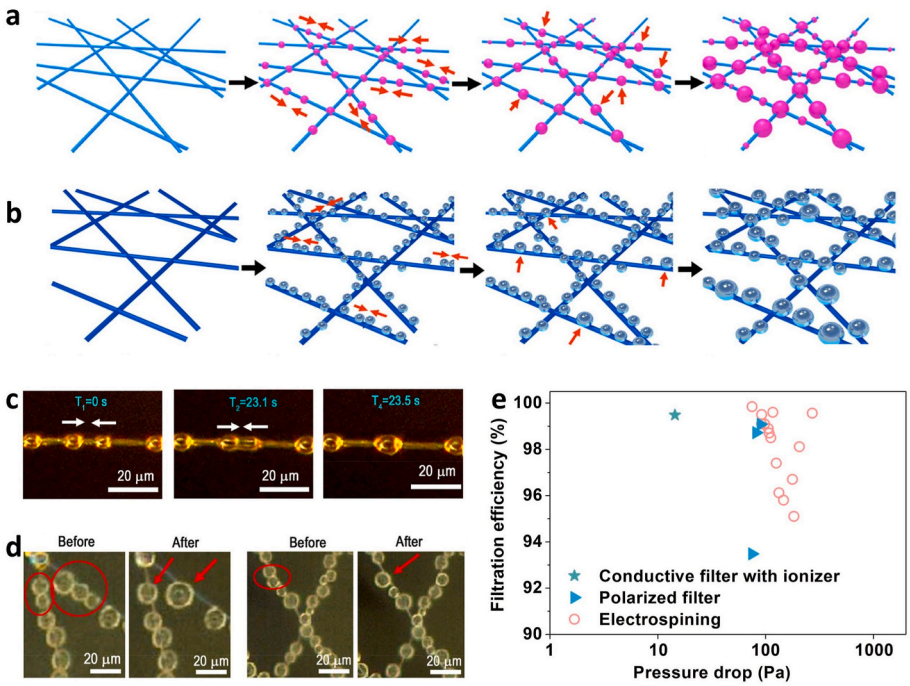

Fig. 11. The schematics of the capture, movement, agglomeration, and growth of **a** wetting and **b** non-wetting droplets on PI nanofibers [167]. The real-time images of the coalescence of adjacent **c** wetting and **d** non-wetting droplets on PI nanofibers. Reproduced with permission from Ref. [167]. Copyright 2018 American Chemical Society. **e** Filtration efficiency for $PM_{2.5}$ and pressure drop of filters strengthened by electrostatic force and tested at ~0.2 m/s air velocity. The data were selected from Tables 2 and 3.

Table 5, the filters charged by induction showed a larger W than uncharged ones, mainly for two reasons: 1) at the beginning, the charged filters have higher filtration efficiency with the same pressure drop, thus enable larger W when tested for the same period of time [107]. 2) The introduction of electrostatic force changes the deposition pattern of particles and slows down the status transition from depth filtration to surface filtration, enabling a slower increase in pressure drop to ensure a larger W at the same ending pressure drop [104]. However, the W of electrostatic strengthened filters can be low, depending on the filter structure. For example, the pressure drop of a membrane-like electret filters could increase from 42 to 250 Pa when W grew from 0 to 0.42 g/m^2 [76], or increase from ~38 to 1000 Pa when W grew from 0 to 10.87 g/m^2 [24]. In HVAC systems, filters with such low W and large ending pressure drop will need frequent replacement. Cotton-like coarse filters, however, have larger pores than those of membrane-like electret filters and can maintain low pressure drops during long-term filtration. Being loaded with ~130 g/m^2 $PM_{2.5}$ in Beijing, the EAA coarse filter accumulatively consumed 56 kWh/m^2 of electricity, only 55% of that was consumed by a commercially obtained electret filter [178]. Shi et al. pushed the testing period record of electrostatic filtration to 216 days, using conventional filters with upstream ionizer on or off. However, the filter only showed high filtration efficiency of 90% for 0.3–0.5 μm particles in the 1–26 days, and the average efficiency decreased to 73% in the 27–116 days and further to 51% in the 117–216 days [139].

Although long-term performance is critical in determining whether the PM filtration technologies can be applied in the built environment, the comprehensive long-term performance of the electrostatic-force strengthened filtration is not fully reported (e.g., many key parameters in Table 5 are not reported). Studies in Table 5 are marked with asterisk if 1) testing time is less than 100 h and the PM holding weight amount is less than 10 g/m^2 or unknown, indicating that the lifetime experiment may not be sufficient for built-environmental application; 2) the ending filtration efficiency is 10% (absolute value) less than the beginning filtration efficiency or 3) the pressure drop increased over 300%, indicating the long-term performance should be improved. Among the reported results, only a few technologies without asterisk marking achieve high efficiency, low pressure drop, and large PM holding capacity filtration at high air velocities. That electrostatic-force strengthened filtration with large PM holding amount, stably high efficiency and low pressure drop is well worth investigating in the future.

6. Summary and perspectives

6.1. Comparison of different technologies

In this study, we summarized the working principle and performance of electrostatic-force strengthened filtration technologies. Regarding whether the PM or the filters are charged, three categories of technology are characterized: (1) singly charging the filters (including one-time charged electret filters and continuously charged ones), (2) singly charging only the PM, and (3) synergistically charging the PM and the filters. In Fig. 12, a well-performance filter should have a high filtration efficiency and low pressure drop at high face air velocity.

Electret air filters, one-time charged before usage, have attracted much attention these years. Though numerous trials have been conducted to improve the charge density on fibers, the key issue of restraining charge dissipation for stably high filtration efficiency is still challenging. Electrospinning is the most widely studied and most effective among all charging methods for electret filters (Fig. 12), while triboelectrification is the simplest one but is rarely reported in applications requiring large air flowrate and large PM holding capacities, such as HVAC filtration and air purifiers.

When singly charging the PM before reaching the filter, the filtration efficiency would significantly increase because of the enhanced dielectrophoresis force. Therefore, relatively high filtration efficiency with low pressure drop at large air velocity can be realized (Fig. 12). However, the PM charging process may produce hazardous ozone, which would increase the risk of respiratory, cardiovascular, and circulatory disease and even mortality [180–182]. Therefore, particulate charging devices should be used with caution in filtration technologies for occupied spaces, unless ozone and other by-product production can be kept below the standard limits.

When both the PM and the filter material are charged, the electrostatic force between them is significantly greater than either the PM or the filter is singly charged, offering the great potential to move towards the aim performance (Fig. 12). Among them, one promising way to obtain high filtration efficiency, minimal air resistance, and long service life (months to years) is precharging PM via corona discharge and polarizing dielectric coarse filters afterward. The strong Coulombic force between the PM and the fibers made the PM easily captured by the fibers with large gaps. Meanwhile, the thick, fluffy and highly porous coarse filters made the air easily pass by, ensuring an ultralow pressure drop at high filtration velocity.

It is worth emphasizing that filtration performance is only comparable when filters/devices are tested at close air face velocity and for the same type of PM with close size distribution (Fig. 12 with PM type and size ignored is only for reference). Besides filtration efficiency, pressure drop and air velocity, other parameters, including power consumption for charging, filter thickness, porosity, and fiber diameter, also determine the filter's long-term performance and cost. However, most research did not mention the additional power that electrostatic filtration devices consumed for PM and filter charging. In this way, a larger QF in which only filtration efficiency and pressure drop are considered may not guarantee better performance. To this end, we strongly recommend using consistent measurement and performance evaluation criteria for electrostatic-force strengthened particulate filtration [183].

Table 4
Performance of reviewed filters for bioaerosol removal. η_i: inactivation efficiency. The "~" means the value is an approximate one given by the reference article, obtained from the figures, indirect calculations or unit conversions.

Ref.	Filter/PM charging method	Filter material	Bioaerosol type	PM size (μm)	η	η_i	Δp (Pa)	v_{air} (m/s)	P (W/m^2)
[31]	Electret/-	PU/*S.flavescens*	*S. epidermidis*	~0.84	95.0%	~99%	~7.84	0.133	-
[175]	Electret/-	chitosan/PA	*E. coli*	-	-	97.2%	-	-	-
[72]	Electret/-	PET/silk	*E. coli*	-	-	94.55%	-	-	-
			S. aureus			94.62%			
[55]	Electret/-	PS	*S. aureus*	~3	99.8%	-	67.4	0.118	-
	Electret/-				99.5%		64.2		
					93.3%		63		
[176]	-/Ionizer	Glass	*E. coli*	-	-	89.8%	-	-	-
[140]	Contact/Ionizer	Ni	*S. aureus*	0.7	98%	~96%	~78.5	~0.052	~79.1
[155]	Contact/Ionizer	PET/Al	*E. coli*	~0.89[a]	99.4%	99.2%	~6	0.034	-
			S. epidermidis		99.6%	98.8%			
[159]	Induced/Corona	PE/PP	*M. parafortuitum*	-	-	99.6%	-	1.37	~2.33
			B. subtilis spores			~0%			~1.19

[a] geometric mean diameter.

Table 5
Long-term performance of reviewed filters. t: testing time, η_{begin} and η_{end}: single-pass filtration efficiency at beginning and end of the testing period, Δp_{begin} and Δp_{end}: pressure drop at beginning and end of testing period. The Ref. columns were marked with * if 1) t < 100 h and $W < 10$ g/m^2 (or unknown W), 2) $\eta_{begin} - \eta_{end} > 10\%$, and 3) $(\Delta p_{end} - \Delta p_{begin})/\Delta p_{begin} > 300\%$. The "~" means the value is an approximate one given by the reference article, obtained from the figures, indirect calculations or unit conversions.

Ref.	Filter/PM charging method	Filter material	L (mm)	t (h)	W (g/m^2)	PM type	PM size (μm)	η_{begin}	η_{end}	Δp_{begin} (Pa)	Δp_{end} (Pa)	v_{air} (m/s)
[165]*	Electret/-	PMMA	-	40 40	-	NaCl	MPPS	97.02% 98.33%	93.35% 86.08%	-	-	0.05
[24]*	Electret/-	PP/PE/MgSt	-	2160 72.5 min	- 10.87	NaCl	0.26[a]	98.94% -	94.90% -	- 37.92	- 1000	0.167
[28]*	Electret/-	PTFE	1.2	380 s 1000 s	-	NaCl Soot	0.5	~89% ~89%	~85% ~89%	90	130	0.083
[30]*	Electret/-	PLA	-	168[b] 4800[b]	-	KCl	0.3–0.5	84% 67% 88.5% 84% 67% 88.5%	~82% ~57% ~81% ~69% ~50% ~67%	27.2 8.5 40.8 27.2 8.5 40.8	-	0.053
[43]*	Electret/-	PS/PAN	-	24[c]	-	NaCl	0.3	99.96%	97.51%	54	-	0.053
[58]*	Electret/-	PVB/Si_3N_4/FPU	-	5	-	NaCl	0.3–0.5	99.99%	99.96%	60.5	63.5	0.053
[44]*	Electret/-	PAN/MOF	-	20	-	NaCl	$PM_{2.5}$ PM_{10}	~88.4% ~84.9%	~94.2% ~99.9%	60.7	-	0.053
[49]*	Electret/-	PS/PAN/CNT	-	~780 s	89.2	NaCl	0.3	96.37%	-	35	~2000	~0.013
[61]*	Electret/-	PI/aramid	-	5 min	-	NaCl	0.4–0.5	94.83%	~99.8%	136	~400	0.1
[37]*	Electret/-	PVDF/PTFE	-	5	-	NaCl	0.3–0.5	94.24% 99.97%	~83.3% ~94.2%	18 57	-	0.053
[32]*	Electret/-	PVDF GO/PVDF	-	1	-	Burning incense	$PM_{2.5}$	93.74% 99.31%	~96.14% ~99.94%	24 35	~29 ~53	0.053
[76]*	Electret/-	PAN/$Ti_3C_2T_x$	-	1	0.42	Burning incense	$PM_{2.5}$	99.7%	~99.7%	42	250	0.053
[179]*	Electret/-	PAN/boehmite	-	48	-	Burning incense	$PM_{2.5}$	99.96%	~99.93%	58	-	0.02
[81]*	Electret/-	PAN PAN/GO	0.1	100	-	Burning incense	$PM_{2.5}$	95.1% 99.6%	84.0% 99.1%	183 117	536 387	0.2
[74]*	Electret/-	PU	-	12	-	Burning cigarette	$PM_{2.5}$	98.92%	>92%	10	-	~0.041
[83]	Electret/-	PTFE/PPS/SiO_2	-	1440	227	NaCl	0.26[a]	89.4%	83.0%	18.6	-	0.053
[104]	−/− Induced/-	PET/PP	300[d]	-	28.4 35.7	Arizona test dust	4	85.2% 98.5%	~99.8% ~99.8%	~120 ~133	375	2.5
[107]*	−/− Induced/-	PAN	0.013	48	2.41 8.43	Burning cigarette	$PM_{2.5}$	86.85% 98.15%	73.56% 90.18%	82	-	0.21
[116]	Contact/ESP	Stainless steel	0.5	1–2	33	Silica	0.5	~97.9%	~98.7%	-	~+986	0.5
[112]*	Contact/Ionizer	PE/Al	0.25	25	~39.1	KCl	0.03–0.4	>99.97%	~99.75%	1.5	26.4	0.025
[114]*	Contact/Ionizer	ZIF-8/Cu/PAN	0.004	15[e]	-	Cu	<1.5	93%	87%	-	-	0.425
[124]*	Induced/ESP	-	90[d]	-	2	Arizona test dust	7.6[a]	92.9%	>99%	~118	~255	2.5
[123]*	Induced/Corona	PE	0.4	-	1.61	Arizona test dust	0.4	~28.2%	~61.5%	8	120	0.1
[158]	Induced/Corona	PP/glass	2 (50[d])	384	-	Ambient	0.3–0.5	60%	77%	~40	~60	0.6
[127]	Induced/Corona	PET	10	458	-	Ambient	0.1–1	~35%	~35%	14.3	31.5	1
[122]	Induced/Corona	PDA/PET	8	240	132.6 173.9	KCl	0.3–0.5	94.80% 94.84%	89.69% 94.79%	-	-	0.4

[a] mass median diameter.
[b] storage time.
[c] working at 90% RH.
[d] pleating height.
[e] 150 cycles of 3 min on and 3 min off.

6.2. Research prospects

Over the last decade, much effort has been devoted to enhancing filtration efficiency and reducing the pressure drop of filtration technologies through the exploitation of nanofibers and electrospun fibers. However, they were usually tested at low air velocity (e.g., <0.1 m/s), or their pressure drops at large air velocity (e.g., >1 m/s) were usually larger than 100 Pa, which should be improved for built-environment applications.

Although the filtration efficiency of synergistically charging the PM and the filter has achieved 99% for 0.3–0.5 μm PM at 1.2 m/s air velocity with a low pressure drop of 21.0 Pa, there are still some problems worth investigating. For example, avoiding electrostatic accumulation and unstable corona discharge is important for long-term performance. As different particulate matter and fibers vary in their ability to get charged, the effectiveness of electrostatic force strengthened filtration in

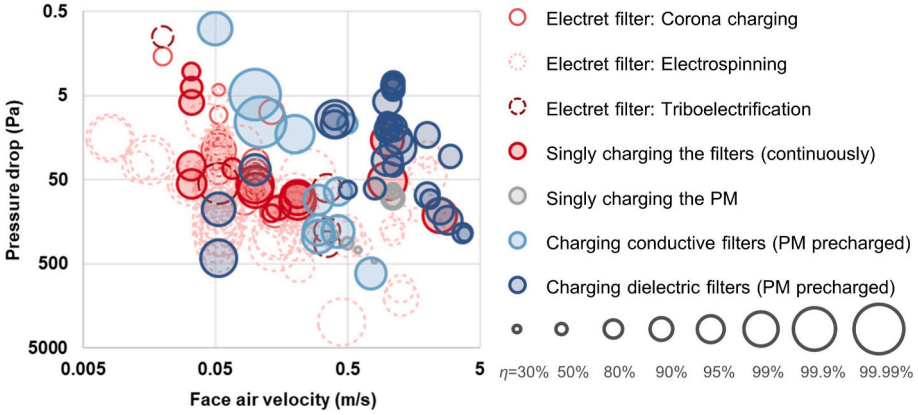

Fig. 12. PM Filtration efficiencies (η, for all PM sizes) and pressure drops of filters strengthened by electrostatic force tested at different face air velocities. $-\ln(1-\eta)$ is represented by the area of the circle. The data were selected from Tables 2 and 3.

different application scenarios can vary considerably. The energy-efficient air cleaning technologies for some special PMs, such as bio-aerosols (especially viruses and allergens), oil droplets, metal particles and microplastic particles, are still worth investigating. Besides, as electrostatic filtration efficiency is strongly influenced by air velocity, it remains a challenge to simultaneously achieve high filtration efficiency and low pressure drop at high air velocity.

Moreover, electrostatic force strengthened filtration is still limited by the need for external power supplies, electrodes, and potential ozone generation. Electret filters, which are one-time charged at the stage of manufacture, have the advantages of being simple, convenient, and safe for human-occupied spaces. The challenges for electret filters are how to avoid filtration degradation due to charge decay and how to fabricate them at low cost and high productivity to facilitate their scale-up application in high-velocity air filtration.

CRediT authorship contribution statement

Enze Tian: Writing – review & editing, Writing – original draft, Visualization, Project administration, Methodology, Investigation, Formal analysis, Data curation, Conceptualization. **Yilun Gao:** Writing – review & editing, Visualization, Data curation. **Jinhan Mo:** Writing – review & editing, Validation, Supervision, Resources, Methodology, Funding acquisition, Conceptualization.

Declaration of competing interest

The authors declare that they have no known competing financial interests or personal relationships that could have appeared to influence the work reported in this paper.

Data availability

Data will be made available on request.

Acknowledgments

The research was supported by the National Natural Science Foundation of China (No. 52078269).

References

[1] M. Loxham, D.E. Davies, S.T. Holgate, The health effects of fine particulate air pollution, Br. Med. J. 367 (2019) l6609, https://doi.org/10.1136/bmj.l6609.
[2] G. Grande, P.L.S. Ljungman, K. Eneroth, T. Bellander, D. Rizzuto, Association between cardiovascular disease and long-term exposure to air pollution with the risk of dementia, JAMA Neurol. 77 (7) (2020) 801–809, https://doi.org/10.1001/jamaneurol.2019.4914.
[3] X. Gao, B. Coull, X. Lin, P. Vokonas, A. Spiro, L. Hou, J. Schwartz, A.A. Baccarelli, Short-term air pollution, cognitive performance and nonsteroidal anti-inflammatory drug use in the Veterans Affairs Normative Aging Study, Nat. Aging 1 (5) (2021) 430–437, https://doi.org/10.1038/s43587-021-00060-4.
[4] World Health Organization, Ambient Air Pollution: A Global Assessment of Exposure and Burden of Disease, 2016.
[5] V.A. Southerland, M. Brauer, A. Mohegh, M.S. Hammer, A. van Donkelaar, R. V. Martin, J.S. Apte, S.C. Anenberg, Global urban temporal trends in fine particulate matter (PM2·5) and attributable health burdens: estimates from global datasets, Lancet Planet. Health 6 (2) (2022) e139–e146, https://doi.org/10.1016/s2542-5196(21)00350-8.
[6] World Health Organization, WHO Global Air Quality Guidelines: Particulate Matter (PM2.5 and PM10), Ozone, Nitrogen Dioxide, Sulfur Dioxide and Carbon Monoxide, 2021.
[7] The United States Environmental Protection Agency, Exposure Factors Handbook, Office of Research and Development, Washington, USA, 1997.
[8] C. Kanaoka, Fine particle filtration technology using fiber as dust collection medium, KONA Powder. Part. J. 36 (2019) 88–113, https://doi.org/10.14356/kona.2019006.
[9] S. Bhangar, N.A. Mullen, S.V. Hering, N.M. Kreisberg, W.W. Nazaroff, Ultrafine particle concentrations and exposures in seven residences in northern California, Indoor Air 21 (2) (2011) 132–144, https://doi.org/10.1111/j.1600-0668.2010.00689.x.
[10] C.N. Davies, The Separation of Airborne Dust and Particles, Proceedings of the Institute of Mechanical Engineers, London, 1952.
[11] R. Thakur, D. Das, A. Das, Electret air filters, Separ. Purif. Rev. 42 (2) (2013) 87–129, https://doi.org/10.1080/15422119.2012.681094.
[12] C.S. Wang, Electrostatic forces in fibrous filters - a review, Powder Technol. 118 (1–2) (2001) 166–170, https://doi.org/10.1016/s0032-5910(01)00307-2.
[13] C. Wang, Y. Otani, Removal of nanoparticles from gas streams by fibrous filters: a review, Ind. Eng. Chem. Res. 52 (1) (2013) 5–17, https://doi.org/10.1021/ie300574m.
[14] B. Stephens, A. Novoselac, J.A. Siegel, The effects of filtration on pressure drop and energy consumption in residential HVAC systems (RP-1299), HVAC R Res. 16 (3) (2010) 273–294, https://doi.org/10.1080/10789669.2010.10390905.
[15] M. Azimian, C. Kuehnle, A. Wiegmann, Design and optimization of fibrous filter media using lifetime multipass simulations, Chem. Eng. Technol. 41 (5) (2018) 928–935, https://doi.org/10.1002/ceat.201700585.
[16] J.F. Montgomery, S.I. Green, S.N. Rogak, K. Bartlett, Predicting the energy use and operation cost of HVAC air filters, Energy Build. 47 (2012) 643–650, https://doi.org/10.1016/j.enbuild.2012.01.001.
[17] C. Lanzerstorfer, F. Neder, R. Schmied, Constant design air flow industrial ventilation systems with regenerative dust filters: economic comparison of fan speed-controlled, air damper controlled and uncontrolled operation, Energy Build. 128 (2016) 503–510, https://doi.org/10.1016/j.enbuild.2016.07.032.
[18] J. Yang, J.G. Siri, J.V. Remais, Q. Cheng, H. Zhang, K.K.Y. Chan, Z. Sun, Y. Zhao, N. Cong, X. Li, W. Zhang, Y. Bai, J. Bi, W. Cai, E.Y.Y. Chan, W. Chen, W. Fan, H. Fu, J. He, H. Huang, J.S. Ji, P. Jia, X. Jiang, M.-P. Kwan, T. Li, X. Li, S. Liang, X. Liang, L. Liang, Q. Liu, Y. Lu, Y. Luo, X. Ma, B. Schwartlander, Z. Shen, P. Shi, J. Su, T. Wu, C. Yang, Y. Yin, Q. Zhang, Y. Zhang, Y. Zhang, B. Xu, P. Gong, The Tsinghua-Lancet Commission on Healthy Cities in China: unlocking the power of cities for a healthy China, Lancet 391 (10135) (2018) 2140–2184, https://doi.org/10.1016/s0140-6736(18)30486-0.
[19] J. Xiao, J. Liang, C. Zhang, Y. Tao, G.-W. Ling, Q.-H. Yang, Advanced materials for capturing particulate matter: progress and perspectives, Small Methods 2 (7) (2018), 1800012, https://doi.org/10.1002/smtd.201800012.
[20] S. Han, J. Kim, S.H. Ko, Advances in air filtration technologies: structure-based and interaction-based approaches, Mater. Today Adv. 9 (2021), 100134, https://doi.org/10.1016/j.mtadv.2021.100134.
[21] H. Zhang, J. Liu, X. Zhang, C. Huang, X. Jin, Online prediction of the filtration performance of polypropylene melt blown nonwovens by blue-colored glow,

J. Appl. Polym. Sci. 135 (10) (2018), 45948, https://doi.org/10.1002/app.45948.
[22] R. Thakur, D. Das, A. Das, Optimization study to improve filtration behaviour of electret filter media, J. Text. Inst. 107 (11) (2016) 1456–1462, https://doi.org/10.1080/00405000.2015.1128207.
[23] C. Liu, Z. Dai, B. He, Q.-F. Ke, The effect of temperature and humidity on the filtration performance of electret melt-blown nonwovens, Materials 13 (21) (2020) 4774, https://doi.org/10.3390/ma13214774.
[24] J. Liu, H. Zhang, H. Gong, X. Zhang, Y. Wang, X. Jin, Polyethylene/polypropylene bicomponent spunbond air filtration materials containing magnesium stearate for efficient fine particle capture, ACS Appl. Mater. Interfaces 11 (43) (2019) 40592–40601, https://doi.org/10.1021/acsami.9b13162.
[25] W.W.F. Leung, Q. Sun, Electrostatic charged nanofiber filter for filtering airborne novel coronavirus (COVID-19) and nano-aerosols, Separ. Purif. Technol. 250 (2020), 116886, https://doi.org/10.1016/j.seppur.2020.116886.
[26] Q. Sun, W.W.-F. Leung, Charged PVDF multi-layer filters with enhanced filtration performance for filtering nano-aerosols, Separ. Purif. Technol. 212 (2019) 854–876, https://doi.org/10.1016/j.seppur.2018.11.063.
[27] C.-T. Wang, S.-T. Lee, L.-Y. Li, J.-Y. Syu, C.-C. Kuo, W.-Y. Lin, A novel-charged fibrous media characterized by higher efficiency and lower pressure drop, Aerosol Sci. Technol. 53 (12) (2019) 1441–1452, https://doi.org/10.1080/02786826.2019.1667477.
[28] W. He, Y.-B. Zhao, F. Jiang, Y. Gu, H. Gao, J. Liu, J. Wang, Filtration performance and charge degradation during particle loading and reusability of charged PTFE needle felt filters, Separ. Purif. Technol. 233 (2020), 116003, https://doi.org/10.1016/j.seppur.2019.116003.
[29] M. Kerner, K. Schmidt, S. Schumacher, V. Puderbach, C. Asbach, S. Antonyuk, Evaluation of electrostatic properties of electret filters for aerosol deposition, Separ. Purif. Technol. 239 (2020), 116548, https://doi.org/10.1016/j.seppur.2020.116548.
[30] J. Zhang, G. Chen, G.S. Bhat, H. Azari, H. Pen, Electret characteristics of melt-blown polylactic acid fabrics for air filtration application, J. Appl. Polym. Sci. 137 (4) (2020), 48309, https://doi.org/10.1002/app.48309.
[31] K.M. Sim, H.-S. Park, G.-N. Bae, J.H. Jung, Antimicrobial nanoparticle-coated electrostatic air filter with high filtration efficiency and low pressure drop, Sci. Total Environ. 533 (2015) 266–274, https://doi.org/10.1016/j.scitotenv.2015.07.003.
[32] M. Chen, J. Jiang, S. Feng, Z.-X. Low, Z. Zhong, W. Xing, Graphene oxide functionalized polyvinylidene fluoride nanofibrous membranes for efficient particulate matter removal, J. Membr. Sci. 635 (2021), 119463, https://doi.org/10.1016/j.memsci.2021.119463.
[33] T.T. Bui, M.K. Shin, S.Y. Jee, D.X. Long, J. Hong, M.-G. Kim, Ferroelectric PVDF nanofiber membrane for high-efficiency PM0.3 air filtration with low air flow resistance, Colloids Surf. A Physicochem. Eng. Asp. 640 (2022), 128418, https://doi.org/10.1016/j.colsurfa.2022.128418.
[34] X. Ding, Y. Li, Y. Si, X. Yin, J. Yu, B. Ding, Electrospun polyvinylidene fluoride/SiO2 nanofibrous membranes with enhanced electret property for efficient air filtration, Compos. Commun. 13 (2019) 57–62, https://doi.org/10.1016/j.coco.2019.02.008.
[35] Z.-X. Huang, X. Liu, X. Zhang, S.-C. Wong, G.G. Chase, J.-P. Qu, A. Baji, Electrospun polyvinylidene fluoride containing nanoscale graphite platelets as electret membrane and its application in air filtration under extreme environment, Polymer 131 (2017) 143–150, https://doi.org/10.1016/j.polymer.2017.10.033.
[36] H. Liu, S.C. Zhang, L.F. Liu, J.Y. Yu, B. Ding, High-performance $PM_{0.3}$ air filters using self-polarized electret nanofiber/nets, Adv. Funct. Mater. 30 (13) (2020), 1909554, https://doi.org/10.1002/adfm.201909554.
[37] S. Wang, X. Zhao, X. Yin, J. Yu, B. Ding, Electret polyvinylidene fluoride nanofibers hybridized by polytetrafluoroethylene nanoparticles for high-efficiency air filtration, ACS Appl. Mater. Interfaces 8 (36) (2016) 23985–23994, https://doi.org/10.1021/acsami.6b08262.
[38] X. Zhao, Y. Li, T. Hua, P. Jiang, X. Yin, J. Yu, B. Ding, Low-resistance dual-purpose air filter releasing negative ions and effectively capturing PM2.5, ACS Appl. Mater. Interfaces 9 (13) (2017) 12054–12063, https://doi.org/10.1021/acsami.7b00351.
[39] T. Dong, Y. Hua, X. Zhu, X. Huang, S. Chi, Y. Liu, C.-W. Lou, J.-H. Lin, Highly efficient and sustainable PM filtration using piezo nanofibrous membrane with gradient shrinking porous network, Separ. Purif. Technol. 289 (2022), 120753, https://doi.org/10.1016/j.seppur.2022.120753.
[40] H. Gao, Y. Yang, O. Akampumuza, J. Hou, H. Zhang, X. Qin, A low filtration resistance three-dimensional composite membrane fabricated via free surface electrospinning for effective PM2.5 capture, Environ. Sci. Nano 4 (4) (2017) 864–875, https://doi.org/10.1039/C6EN00696E.
[41] Y. Yang, S. Zhang, X. Zhao, J. Yu, B. Ding, Sandwich structured polyamide-6/polyacrylonitrile nanonets/bead-on-string composite membrane for effective air filtration, Separ. Purif. Technol. 152 (2015) 14–22, https://doi.org/10.1016/j.seppur.2015.08.005.
[42] M. Zhou, Q. Fan, Z. Quan, H. Zhang, L. Wang, X. Qin, R. Wang, J. Yu, Mass production of polyacrylonitrile sub-micron fibrous webs with different aligned degrees via free surface electrospinning for air purification, Textil. Res. J. (2021), https://doi.org/10.1177/00405175211010688.
[43] R.-R. Cai, S.-Z. Li, L.-Z. Zhang, Y. Lei, Fabrication and performance of a stable micro/nano composite electret filter for effective PM2.5 capture, Sci. Total Environ. 725 (2020), 138297, https://doi.org/10.1016/j.scitotenv.2020.138297.
[44] M. Lee, G.P. Ojha, H.J. Oh, T. Kim, H.Y. Kim, Copper//terbium dual metal organic frameworks incorporated side-by-side electrospun nanofibrous membrane: a novel tactics for an efficient adsorption of particulate matter and luminescence property, J. Colloid Interface Sci. 578 (2020) 155–163, https://doi.org/10.1016/j.jcis.2020.05.113.
[45] J. Li, D. Zhang, X. Jiang, X. Zhao, R. Hu, Y. Zhong, H. Zhu, Nest-like multilevel structured graphene oxide-on-polyacrylonitrile membranes for highly efficient filtration of ultrafine particles, J. Materiomics 5 (3) (2019) 422–427, https://doi.org/10.1016/j.jmat.2019.02.011.
[46] N. Wang, Y. Yang, S.S. Al-Deyab, M. El-Newehy, J. Yu, B. Ding, Ultra-light 3D nanofibre-nets binary structured nylon 6-polyacrylonitrile membranes for efficient filtration of fine particulate matter, J. Mater. Chem. 3 (47) (2015) 23946–23954, https://doi.org/10.1039/C5TA06543G.
[47] Y. Liu, M. Park, B. Ding, J. Kim, M. El-Newehy, S.S. Al-Deyab, H.Y. Kim, Facile electrospun polyacrylonitrile/poly(acrylic acid) nanofibrous membranes for high efficiency particulate air filtration, Fibers Polym. 16 (3) (2015) 629–633, https://doi.org/10.1007/s12221-015-0629-1.
[48] B. Robert, G. Nallathambi, Highly oriented poly (m-phenylene isophthalamide)/polyacrylonitrile based coaxial nanofibers integrated with electrospun polyacrylonitrile-silver nanoparticle: application in air filtration of particulate and microbial contaminants, J. Appl. Polym. Sci. 139 (23) (2022), e52294, https://doi.org/10.1002/app.52294.
[49] W. Shao, W. Yue, G. Ren, C. Cui, J. Xiong, L. Wang, T. Lu, W. Bu, F. Liu, J. He, Electrospun PS/PAN nanofiber membranes formed from doped carbon nanotubes with a fluffy and multi-scale construction for air-filtration materials, Fibers Polym. 23 (2022) 1197–1205, https://doi.org/10.1007/s12221-022-4652-8.
[50] Z. Wang, Z. Pan, Preparation of hierarchical structured nano-sized/porous poly (lactic acid) composite fibrous membranes for air filtration, Appl. Surf. Sci. 356 (2015) 1168–1179, https://doi.org/10.1016/j.apsusc.2015.08.211.
[51] A. Nicosia, W. Gieparda, J. Foksowicz-Flaczyk, J. Walentowska, D. Wesolek, B. Vazquez, F. Prodi, F. Belosi, Air filtration and antimicrobial capabilities of electrospun PLA/PHB containing ionic liquid, Separ. Purif. Technol. 154 (2015) 154–160, https://doi.org/10.1016/j.seppur.2015.09.037.
[52] J. Song, B. Zhang, Z. Lu, Z. Xing, T. Liu, W. Wei, Q. Zia, K. Pan, R.H. Gong, L. Bian, Y. Li, J. Li, Hierarchical porous poly(L-lactic acid) nanofibrous membrane for ultrafine particulate aerosol filtration, ACS Appl. Mater. Interfaces 11 (49) (2019) 46261–46268, https://doi.org/10.1021/acsami.9b18083.
[53] L. Deng, P. Zhang, W. Zhang, R. Zhu, Y. Yan, High filtration efficiency fluffy material: nano-fiber constructing gradient structure on recycled curved PET micro-fibers web, SN Appl. Sci. 1 (2) (2019) 190, https://doi.org/10.1007/s42452-019-0209-x.
[54] S. Roh, S. Kim, J. Kim, Facile functionalization via plasma-enhanced chemical vapor deposition for the effective filtration of oily aerosol, Polymers 11 (9) (2019) 1490, https://doi.org/10.3390/polym11091490.
[55] S. Jung, J. An, H. Na, J. Kim, Surface energy of filtration media influencing the filtration performance against solid particles, oily aerosol, and bacterial aerosol, Polymers 11 (6) (2019) 935, https://doi.org/10.3390/polym11060935.
[56] Y. Li, J. Ming, D. Yuan, X. Ning, High-temperature bearable polysulfonamide/polyurethane composite nanofibers' membranes for filtration application, Macromol. Mater. Eng. 306 (7) (2021), 2100081, https://doi.org/10.1002/mame.202100081.
[57] H. Wan, N. Wang, J. Yang, Y. Si, K. Chen, B. Ding, G. Sun, M. El-Newehy, S.S. Al-Deyab, J. Yu, Hierarchically structured polysulfone/titania fibrous membranes with enhanced air filtration performance, J. Colloid Interface Sci. 417 (2014) 18–26, https://doi.org/10.1016/j.jcis.2013.11.009.
[58] P. Jiang, X. Zhao, Y. Li, Y. Liao, T. Hua, X. Yin, J. Yu, B. Ding, Moisture and oily molecules stable nanofibrous electret membranes for effectively capturing PM2.5, Compos. Commun. 6 (2017) 34–40, https://doi.org/10.1016/j.coco.2017.08.004.
[59] N. Wang, A. Raza, Y. Si, J. Yu, G. Sun, B. Ding, Tortuously structured polyvinyl chloride/polyurethane fibrous membranes for high-efficiency fine particulate filtration, J. Colloid Interface Sci. 398 (2013) 240–246, https://doi.org/10.1016/j.jcis.2013.02.019.
[60] S. Chattopadhyay, T.A. Hatton, G.C. Rutledge, Aerosol filtration using electrospun cellulose acetate fibers, J. Mater. Sci. 51 (1) (2016) 204–217, https://doi.org/10.1007/s10853-015-9286-4.
[61] L. Li, L.M. Shang, Y.X. Li, C.F. Yang, Three-layer composite filter media containing electrospun polyimide nanofibers for the removal of fine particles, Fibers Polym. 18 (4) (2017) 749–757, https://doi.org/10.1007/s12221-017-1094-9.
[62] X. Li, N. Wang, G. Fan, J. Yu, J. Gao, G. Sun, B. Ding, Electreted polyetherimide-silica fibrous membranes for enhanced filtration of fine particles, J. Colloid Interface Sci. 439 (2015) 12–20, https://doi.org/10.1016/j.jcis.2014.10.014.
[63] B. Liu, S. Zhang, X. Wang, J. Yu, B. Ding, Efficient and reusable polyamide-56 nanofiber/nets membrane with bimodal structures for air filtration, J. Colloid Interface Sci. 457 (2015) 203–211, https://doi.org/10.1016/j.jcis.2015.07.019.
[64] C. Wang, S. Wu, M. Jian, J. Xie, L. Xu, X. Yang, Q. Zheng, Y. Zhang, Silk nanofibers as high efficient and lightweight air filter, Nano Res. 9 (9) (2016) 2590–2597, https://doi.org/10.1007/s12274-016-1145-3.
[65] R. Al-Attabi, L.F. Dumee, J.A. Schutz, Y. Morsi, Pore engineering towards highly efficient electrospun nanofibrous membranes for aerosol particle removal, Sci. Total Environ. 625 (2018) 706–715, https://doi.org/10.1016/j.scitotenv.2017.12.342.
[66] K.S. Han, S. Lee, M. Kim, P. Park, M.H. Lee, J. Nah, Electrically activated ultrathin PVDF-TrFE air filter for high-efficiency PM1.0 filtration, Adv. Funct. Mater. 29 (37) (2019), 1903633, https://doi.org/10.1002/adfm.201903633.
[67] F. Mueller, S. Zainuddin, T. Scheibel, Roll-to-roll production of spider silk nanofiber nonwoven meshes using centrifugal electrospinning for filtration

applications, Molecules 25 (23) (2020) 5540, https://doi.org/10.3390/molecules25235540.
[68] S. Jokisch, M. Neuenfeldt, T. Scheibel, Silk-based fine dust filters for air filtration, Adv. Sustain. Syst. 1 (10) (2017), 1700079, https://doi.org/10.1002/adsu.201700079.
[69] I. Kulmala, T. Zweglinski, M. Smolarkiewicz, H. Salmela, T. Kalliohaka, A. Taipale, J. Kataja, V. Makipaa, Effect of enhanced supply air filtration in buildings on protecting citizens from environmental radioactive particles, Build. Simulat. 13 (4) (2020) 865–872, https://doi.org/10.1007/s12273-020-0621-6.
[70] D. Li, Y. Shen, L. Wang, F. Liu, B. Deng, Q. Liu, Hierarchical structured polyimide-silica hybrid nano/microfiber filters welded by solvent vapor for air filtration, Polymers 12 (11) (2020) 2494, https://doi.org/10.3390/polym12112494.
[71] X. Yang, Y. Pu, S. Li, X. Liu, Z. Wang, D. Yuan, X. Ning, Electrospun polymer composite membrane with superior thermal stability and excellent chemical resistance for high-efficiency PM2.5 capture, ACS Appl. Mater. Interfaces 11 (46) (2019) 43188–43199, https://doi.org/10.1021/acsami.9b15219.
[72] A.O. Siskova, K. Mosnackova, J. Hruza, J. Frajova, A. Opalek, M. Buckova, K. Kozics, P. Peer, A.E. Andicsova, Electrospun poly(ethylene terephthalate)/silk fibroin composite for filtration application, Polymers 13 (15) (2021) 2499, https://doi.org/10.3390/polym13152499.
[73] J. Matulevicius, L. Kliucininkas, T. Prasauskas, D. Buivydiene, D. Martuzevicius, The comparative study of aerosol filtration by electrospun polyamide, polyvinyl acetate, polyacrylonitrile and cellulose acetate nanofiber media, J. Aerosol Sci. 92 (2016) 27–37, https://doi.org/10.1016/j.jaerosci.2015.10.006.
[74] R.W. Chen, X.W. Zhang, P.J. Wang, K.H. Xie, J.W. Jian, Y.J. Zhang, J.R. Zhang, Y. L. Yuan, P.D. Na, M.Q. Yi, J. Xu, Transparent thermoplastic polyurethane air filters for efficient electrostatic capture of particulate matter pollutants, Nanotechnology 30 (1) (2019), 015703, https://doi.org/10.1088/1361-6528/aae611.
[75] X. Gao, J. Gou, L. Zhang, S. Duan, C. Li, A silk fibroin based green nano-filter for air filtration, RSC Adv. 8 (15) (2018) 8181–8189, https://doi.org/10.1039/c7ra12879g.
[76] X. Gao, Z.-K. Li, J. Xue, Y. Qian, L.-Z. Zhang, J. Caro, H. Wang, Titanium carbide Ti3C2Tx (MXene) enhanced PAN nanofiber membrane for air purification, J. Membr. Sci. 586 (2019) 162–169, https://doi.org/10.1016/j.memsci.2019.05.058.
[77] C. Liu, P.-C. Hsu, H.-W. Lee, M. Ye, G. Zheng, N. Liu, W. Li, Y. Cui, Transparent air filter for high-efficiency PM2.5 capture, Nat. Commun. 6 (1) (2015) 6205, https://doi.org/10.1038/ncomms7205.
[78] K. Liu, C. Liu, P.-C. Hsu, J. Xu, B. Kong, T. Wu, R. Zhang, G. Zhou, W. Huang, J. Sun, Y. Cui, Core-shell nanofibrous materials with high particulate matter removal efficiencies and thermally triggered flame retardant properties, ACS Cent. Sci. 4 (7) (2018) 894–898, https://doi.org/10.1021/acscentsci.8b00285.
[79] J. Xu, C. Liu, P.-C. Hsu, K. Liu, R. Zhang, Y. Liu, Y. Cui, Roll-to-roll transfer of electrospun nanofiber film for high-efficiency transparent air filter, Nano Lett. 16 (2) (2016) 1270–1275, https://doi.org/10.1021/acs.nanolett.5b04596.
[80] Q.J. Zhang, Q. Li, T.M. Young, D.P. Harper, S.Q. Wang, A novel method for fabricating an electrospun poly(vinyl alcohol)/cellulose nanocrystals composite nanofibrous filter with low air resistance for high-efficiency filtration of particulate matter, ACS Sustain. Chem. Eng. 7 (9) (2019) 8706–8714, https://doi.org/10.1021/acssuschemeng.9b00605.
[81] C. Zhang, L. Yao, Z. Yang, E.S.-W. Kong, X. Zhu, Y. Zhang, Graphene oxide-modified polyacrylonitrile nanofibrous membranes for efficient air filtration, ACS Appl. Nano Mater. 2 (6) (2019) 3916–3924, https://doi.org/10.1021/acsanm.9b00806.
[82] H. Dai, X. Liu, C. Zhang, K. Ma, Y. Zhang, Electrospinning polyacrylonitrile/graphene oxide/polyimide nanofibrous membranes for high-efficiency PM2.5 filtration, Separ. Purif. Technol. 276 (2021), 119243, https://doi.org/10.1016/j.seppur.2021.119243.
[83] Y. Wang, Y. Xu, D. Wang, Y. Zhang, X. Zhang, J. Liu, Y. Zhao, C. Huang, X. Jin, Polytetrafluoroethylene/polyphenylene sulfide needle-punched triboelectric air filter for efficient particulate matter removal, ACS Appl. Mater. Interfaces 11 (51) (2019) 48437–48449, https://doi.org/10.1021/acsami.9b18341.
[84] D. Park, M. Kim, S. Lee, I.-J. Yoon, K. Lee, M.H. Lee, J. Nah, Light-permeable air filter with self-polarized Nylon-11 nanofibers for enhanced trapping of particulate matters, Adv. Mater. Interfac. 6 (5) (2019), 1801832, https://doi.org/10.1002/admi.201801832.
[85] J.A. Giacometti, O.N. Oliveira, Corona charging of polymers, IEEE Trans. Electr. Insul. 27 (5) (1992) 924–943, https://doi.org/10.1109/14.256470.
[86] R. Thakur, D. Das, A. Das, Study of charge decay in corona-charged fibrous electrets, Fibers Polym. 15 (7) (2014) 1436–1443, https://doi.org/10.1007/s12221-014-1436-9.
[87] J. Xue, T. Wu, Y. Dai, Y. Xia, Electrospinning and electrospun nanofibers: methods, materials, and applications, Chem. Rev. 119 (8) (2019) 5298–5415, https://doi.org/10.1021/acs.chemrev.8b00593.
[88] R.R. Cai, L.Z. Zhang, A.B. Bao, PM collection performance of electret filters electrospun with different dielectric materials-a numerical modeling and experimental study, Build. Environ. 131 (2018) 210–219, https://doi.org/10.1016/j.buildenv.2017.12.036.
[89] Q. Li, Y. Xu, H. Wei, X. Wang, An electrospun polycarbonate nanofibrous membrane for high efficiency particulate matter filtration, RSC Adv. 6 (69) (2016) 65275–65281, https://doi.org/10.1039/c6ra12320a.
[90] J.N. Israelachvili, Intermolecular and Surface Forces, Elsevier Science, 2011.
[91] Y. Bai, C.B. Han, C. He, G.Q. Gu, J.H. Nie, J.J. Shao, T.X. Xiao, C.R. Deng, Z. L. Wang, Washable multilayer triboelectric air filter for efficient particulate matter PM2.5 removal, Adv. Funct. Mater. 28 (15) (2018), 1706680, https://doi.org/10.1002/adfm.201706680.
[92] N. Wang, Y. Si, N. Wang, G. Sun, M. El-Newehy, S.S. Al-Deyab, B. Ding, Multilevel structured polyacrylonitrile/silica nanofibrous membranes for high-performance air filtration, Separ. Purif. Technol. 126 (2014) 44–51, https://doi.org/10.1016/j.seppur.2014.02.017.
[93] Y. Zhang, S. Yuan, X. Feng, H. Li, J. Zhou, B. Wang, Preparation of nanofibrous metal–organic framework filters for efficient air pollution control, J. Am. Chem. Soc. 138 (18) (2016) 5785–5788, https://doi.org/10.1021/jacs.6b02553.
[94] T. Xia, Y. Bian, S. Shi, L. Zhang, C. Chen, Influence of nanofiber window screens on indoor PM(2.5)of outdoor origin and ventilation rate: an experimental and modeling study, Build. Simulat. 13 (4) (2020) 873–886, https://doi.org/10.1007/s12273-020-0622-5.
[95] J. Liu, T. Jiang, X. Li, Z.L. Wang, Triboelectric filtering for air purification, Nanotechnology 30 (29) (2019), 292001, https://doi.org/10.1088/1361-6528/ab0e34.
[96] Y. Hu, Y. Wang, S. Tian, A. Yu, L. Wan, J. Zhai, Performance-enhanced and washable triboelectric air filter based on polyvinylidene fluoride/UiO-66 composite nanofiber membrane, Macromol. Mater. Eng. 306 (8) (2021), 2100128, https://doi.org/10.1002/mame.202100128.
[97] X. He, H. Zou, Z. Geng, X. Wang, W. Ding, F. Hu, Y. Zi, C. Xu, S.L. Zhang, H. Yu, M. Xu, W. Zhang, C. Lu, Z.L. Wang, A hierarchically nanostructured cellulose fiber-based triboelectric nanogenerator for self-powered healthcare products, Adv. Funct. Mater. 28 (45) (2018), 1805540, https://doi.org/10.1002/adfm.201805540.
[98] G. Liu, J. Nie, C. Han, T. Jiang, Z. Yang, Y. Pang, L. Xu, T. Guo, T. Bu, C. Zhang, Z. L. Wang, Self-powered electrostatic adsorption face mask based on a triboelectric nanogenerator, ACS Appl. Mater. Interfaces 10 (8) (2018) 7126–7133, https://doi.org/10.1021/acsami.7b18732.
[99] P.S. Kasbe, H. Gade, S. Liu, G.G. Chase, W. Xu, Ultrathin polydopamine-graphene oxide hybrid coatings on polymer filters with improved filtration performance and functionalities, ACS Appl. Bio Mater. 4 (6) (2021) 5180–5188, https://doi.org/10.1021/acsabm.1c00367.
[100] H.J. Kim, S.J. Park, D.I. Kim, S. Lee, O.S. Kwon, I.K. Kim, Moisture effect on particulate matter filtration performance using electro-spun nanofibers including density functional theory analysis, Sci. Rep. 9 (2019) 7015, https://doi.org/10.1038/s41598-019-43127-4.
[101] P.C. Raynor, B.G. Kim, G. Ramachandran, M.R. Strommen, J.H. Horns, A. J. Streifel, Collection of biological and non-biological particles by new and used filters made from glass and electrostatically charged synthetic fibers, Indoor Air 18 (1) (2008) 51–62, https://doi.org/10.1111/j.1600-0668.2007.00504.x.
[102] Z.F. Xia, S.S. Ma, X.L. Qiu, Y.H. Wu, F.P. Wang, Influence of porosity on the stability of charge and piezoelectricity for porous polytetrafluoroethylene film electrets, J. Electrost. 59 (1) (2003) 57–69, https://doi.org/10.1016/s0304-3886(03)00089-5.
[103] Z. Shao, J. Jiang, X. Wang, W. Li, L. Fang, G. Zheng, Self-powered electrospun composite nanofiber membrane for highly efficient air filtration, Nanomaterials 10 (9) (2020) 1706, https://doi.org/10.3390/nano10091706.
[104] K.-S. Lee, N. Hasolli, J.-R. Lee, K.-D. Kim, S.-D. Kim, Y.-O. Park, J. Hwang, Dust loading performance of a non-electret HVAC filter module in the presence of an external electric field, Separ. Purif. Technol. 250 (2020), 117204, https://doi.org/10.1016/j.seppur.2020.117204.
[105] Q. Wang, F. Khan, L. Wei, H. Shen, C. Zhang, Q. Jiang, Y. Qiu, Filtration properties of carbon woven fabric filters supplied with high voltage for removal of PM 1.0 particles, Separ. Purif. Technol. 177 (2017) 40–48, https://doi.org/10.1016/j.seppur.2016.11.054.
[106] L. Wang, Y. Bian, C.K. Lim, Z. Niu, P.K.H. Lee, C. Chen, L. Zhang, W.A. Daoud, Y. Zi, Tribo-charge enhanced hybrid air filter masks for efficient particulate matter capture with greatly extended service life, Nano Energy 85 (2021), 106015, https://doi.org/10.1016/j.nanoen.2021.106015.
[107] C.X. Li, S.Y. Kuang, Y.H. Chen, Z.L. Wang, C. Li, G. Zhu, In situ active poling of nanofiber networks for gigantically enhanced particulate filtration, ACS Appl. Mater. Interfaces 10 (29) (2018) 24332–24338, https://doi.org/10.1021/acsami.8b07203.
[108] G.Q. Gu, C.B. Han, C.X. Lu, C. He, T. Jiang, Z.L. Gao, C.J. Li, Z.L. Wang, Triboelectric nanogenerator enhanced nanofiber air filters for efficient particulate matter removal, ACS Nano 11 (6) (2017) 6211–6217, https://doi.org/10.1021/acsnano.7b02321.
[109] J.H. Park, K.Y. Yoon, J.H. Hwang, Removal of submicron particles using a carbon fiber ionizer-assisted medium air filter in a heating, ventilation, and air-conditioning (HVAC) system, Build. Environ. 46 (8) (2011) 1699–1708, https://doi.org/10.1016/j.buildenv.2011.02.010.
[110] Z.B. Feng, Z.W. Long, T. Yu, Filtration characteristics of fibrous filter following an electrostatic precipitator, J. Electrost. 83 (2016) 52–62, https://doi.org/10.1016/j.elstat.2016.07.009.
[111] I.E. Agranovski, R. Huang, O.V. Pyankov, I.S. Altman, S.A. Grinshpun, Enhancement of the performance of low-efficiency HVAC filters due to continuous unipolar ion emission, Aerosol Sci. Technol. 40 (11) (2006) 963–968, https://doi.org/10.1080/02786820600833203.
[112] D.Y. Choi, S.H. Jung, D.K. Song, E.J. An, D. Park, T.O. Kim, J.H. Jung, H.M. Lee, Al-coated conductive fibrous filter with low pressure drop for efficient electrostatic capture of ultrafine particulate pollutants, ACS Appl. Mater. Interfaces 9 (19) (2017) 16495–16504, https://doi.org/10.1021/acsami.7b03047.
[113] D.Y. Choi, E.J. An, S.H. Jung, D.K. Song, Y.S. Oh, H.W. Lee, H.M. Lee, Al-coated conductive fiber filters for high-efficiency electrostatic filtration: effects of

electrical and fiber structural properties, Sci. Rep. 8 (2018) 1–10, https://doi.org/10.1038/s41598-018-23960-9.
[114] M.-W. Kim, Y.-I. Kim, C. Park, A. Aldalbahi, H.S. Alanazi, S. An, A.L. Yarin, S. S. Yoon, Reusable and durable electrostatic air filter based on hybrid metallized microfibers decorated with metal-organic-framework nanocrystals, J. Mater. Sci. Technol. 85 (2021) 44–55, https://doi.org/10.1016/j.jmst.2020.12.065.
[115] E. Tian, J. Mo, X. Li, Electrostatically assisted metal foam coarse filter with small pressure drop for efficient removal of fine particles: effect of filter medium, Build. Environ. 144 (2018) 419–426, https://doi.org/10.1016/j.buildenv.2018.08.026.
[116] S. Kim, C. Sioutas, M. Chang, Electrostatic enhancement of the collection efficiency of stainless steel fiber filters, Aerosol Sci. Technol. 32 (3) (2000) 197–213, https://doi.org/10.1080/027868200303731.
[117] J. Mermelstein, S. Kim, C. Sioutas, Electrostatically enhanced stainless steel filters: effect of filter structure and pore size on particle removal, Aerosol Sci. Technol. 36 (1) (2002) 62–75, https://doi.org/10.1080/027868202753339087.
[118] S. Jeong, H. Cho, S. Han, P. Won, H. Lee, S. Hong, J. Yeo, J. Kwon, S.H. Ko, High efficiency, transparent, reusable, and active PM2.5 filters by hierarchical Ag nanowire percolation network, Nano Lett. 17 (7) (2017) 4339–4346, https://doi.org/10.1021/acs.nanolett.7b01404.
[119] W.-R. Huang, Z. He, J.-L. Wang, J.-W. Liu, S.-H. Yu, Mass production of nanowire-nylon flexible transparent smart windows for PM2.5 capture, iScience 12 (2019) 333–341, https://doi.org/10.1016/j.isci.2019.01.014.
[120] Y.-H. Joe, J. Shim, W.G. Shin, H.-S. Park, Effects of an external electric field on the collection efficiency of air filters: filtration mechanisms with an external e-field, Aerosol Sci. Technol. 51 (12) (2017) 1409–1418, https://doi.org/10.1080/02786826.2017.1361014.
[121] N.S. Sambudi, H.J. Choi, M.H. Lee, K. Cho, Capture of ultrafine particles using a film-type electret filter with a unipolar charger, Aerosol Air Qual. Res. 17 (2) (2017) 626–635, https://doi.org/10.4209/aaqr.2016.03.0104.
[122] E. Tian, Q. Yu, Y. Gao, H. Wang, C. Wang, Y. Zhang, B. Li, M. Zhu, J. Mo, G. Xu, J. Li, Ultralow resistance two-stage electrostatically assisted air filtration by polydopamine coated PET coarse filter, Small 17 (33) (2021), 2102051, https://doi.org/10.1002/smll.202102051.
[123] Z.B. Feng, Z.W. Long, J.H. Mo, Experimental and theoretical study of a novel electrostatic enhanced air filter (EEAF) for fine particles, J. Aerosol Sci. 102 (2016) 41–54, https://doi.org/10.1016/j.jaerosci.2016.08.012.
[124] J.K. Lee, S.C. Kim, J.H. Shin, J.E. Lee, J.H. Ku, H.S. Shin, Performance evaluation of electrostatically augmented air filters coupled with a corona precharger, Aerosol Sci. Technol. 35 (4) (2001) 785–791, https://doi.org/10.1080/027868201753227334.
[125] Y. Gao, E. Tian, J. Mo, Electrically responsive coarse filters endowed by high-dielectric-constant surface coatings toward efficient removal of ultrafine particles and ozone, ACS ES&T Eng. 1 (10) (2021) 1449–1459, https://doi.org/10.1021/acsestengg.1c00186.
[126] E. Tian, F. Xia, J. Wu, Y. Zhang, J. Li, H. Wang, J. Mo, Electrostatic air filtration by multifunctional dielectric heterocaking filters with ultralow pressure drop, ACS Appl. Mater. Interfaces 12 (26) (2020) 29383–29392, https://doi.org/10.1021/acsami.0c07447.
[127] E. Tian, J. Mo, Z. Long, H. Luo, Y. Zhang, Experimental study of a compact electrostatically assisted air coarse filter for efficient particle removal: synergistic particle charging and filter polarizing, Build. Environ. 135 (2018) 153–161, https://doi.org/10.1016/j.buildenv.2018.03.002.
[128] E. Tian, J. Mo, Toward energy saving and high efficiency through an optimized use of a PET coarse filter: the development of a new electrostatically assisted air filter, Energy Build. 186 (2019) 276–283, https://doi.org/10.1016/j.enbuild.2019.01.021.
[129] J. Mo, Y. Gu, E. Tian, Efficiently remove submicron particles by a novel foldable electrostatically assisted air coarse filter, Separ. Purif. Technol. 288 (2022), 120631, https://doi.org/10.1016/j.seppur.2022.120631.
[130] R. Orlando, Y. Gao, P. Fojan, J. Mo, A. Afshari, Filtration performance of ultrathin electrospun cellulose acetate filters doped with TiO2 and activated charcoal, Buildings 11 (11) (2021) 557, https://doi.org/10.3390/buildings11110557.
[131] M.-W. Kim, S. An, H. Seok, S.S. Yoon, A.L. Yarin, Electrostatic transparent air filter membranes composed of metallized microfibers for particulate removal, ACS Appl. Mater. Interfaces 11 (29) (2019) 26323–26332, https://doi.org/10.1021/acsami.9b05686.
[132] F.-R. Fan, Z.-Q. Tian, Z. Lin Wang, Flexible triboelectric generator, Nano Energy 1 (2) (2012) 328–334, https://doi.org/10.1016/j.nanoen.2012.01.004.
[133] W. Yang, J. Chen, G. Zhu, J. Yang, P. Bai, Y. Su, Q. Jing, X. Cao, Z.L. Wang, Harvesting energy from the natural vibration of human walking, ACS Nano 7 (12) (2013) 11317–11324, https://doi.org/10.1021/nn405175z.
[134] Y. Xie, S. Wang, L. Lin, Q. Jing, Z.-H. Lin, S. Niu, Z. Wu, Z.L. Wang, Rotary triboelectric nanogeneratorbased on a hybridized mechanism for harvesting wind energy, ACS Nano 7 (8) (2013) 7119–7125, https://doi.org/10.1021/nn402477h.
[135] L.M. Zhang, C.B. Han, T. Jiang, T. Zhou, X.H. Li, C. Zhang, Z.L. Wang, Multilayer wavy-structured robust triboelectric nanogenerator for harvesting water wave energy, Nano Energy 22 (2016) 87–94, https://doi.org/10.1016/j.nanoen.2016.01.009.
[136] Y. Bian, T. Jiang, T. Xiao, W. Gong, X. Cao, Z. Wang, Z.L. Wang, Triboelectric nanogenerator tree for harvesting wind energy and illuminating in subway tunnel, Adv. Mater. Technol. 3 (3) (2018), 1700317, https://doi.org/10.1002/admt.201700317.
[137] G.Q. Gu, C.B. Han, J.J. Tian, T. Jiang, C. He, C.X. Lu, Y. Bai, J.H. Nie, Z. Li, Z. L. Wang, Triboelectric nanogenerator enhanced multilayered antibacterial nanofiber air filters for efficient removal of ultrafine particulate matter, Nano Res. 11 (8) (2018) 4090–4101, https://doi.org/10.1007/s12274-018-1992-1.
[138] K. Ko, S.-C. Yang, Magnetoelectric membrane filters of poly(vinylidene fluoride)/cobalt ferrite oxide for effective capturing of particulate matter, Polymers 12 (11) (2020) 2601, https://doi.org/10.3390/polym12112601.
[139] B. Shi, L. Ekberg, Ionizer assisted air filtration for collection of submicron and ultrafine particles-evaluation of long-term performance and influencing factors, Environ. Sci. Technol. 49 (11) (2015) 6891–6898, https://doi.org/10.1021/acs.est.5b00974.
[140] C.G. Woo, H.-J. Kim, Y.-J. Kim, B. Han, Enhanced antimicrobial activity on non-conducting and conducting air filters by using air ions and grapefruit seed extract, Aerosol Air Qual. Res. 17 (7) (2017) 1917–1924, https://doi.org/10.4209/aaqr.2016.10.0466.
[141] A. Afshari, L. Ekberg, L. Forejt, J. Mo, S. Rahimi, J. Siegel, W. Chen, P. Wargocki, S. Zurami, J. Zhang, Electrostatic precipitators as an indoor air cleaner-a literature review, Sustainability 12 (21) (2020) 8774, https://doi.org/10.3390/su12218774.
[142] A. Mizuno, Electrostatic precipitation, IEEE Trans. Dielectr. Electr. Insul. 7 (5) (2000) 615–624, https://doi.org/10.1109/94.879357.
[143] J. Mo, E. Tian, J. Pan, New electrostatic precipitator with dielectric coatings to efficiently and safely remove sub-micro particles in the building environment, Sustain. Cities Soc. 55 (2020), 102063, https://doi.org/10.1016/j.scs.2020.102063.
[144] M.S. Zuraimi, M. Vuotari, G. Nilsson, R. Magee, B. Kemery, C. Alliston, Impact of dust loading on long term portable air cleaner performance, Build. Environ. 112 (2017) 261–269, https://doi.org/10.1016/j.buildenv.2016.11.001.
[145] A. Jaworek, A.T. Sobczyk, A. Krupa, A. Marchewicz, T. Czech, L. Sliwinski, Hybrid electrostatic filtration systems for fly ash particles emission control. A review, Sep. Purif. Technol. 213 (2019) 283–302, https://doi.org/10.1016/j.seppur.2018.12.011.
[146] G.M. Tu, Q. Song, Q. Yao, Experimental and numerical study of particle deposition on perforated plates in a hybrid electrostatic filter precipitator, Powder Technol. 321 (2017) 143–153, https://doi.org/10.1016/j.powtec.2017.08.021.
[147] M.V. Rodrigues, M.A.S. Barrozo, J.A.S. Goncalves, J.R. Coury, Effect of particle electrostatic charge on aerosol filtration by a fibrous filter, Powder Technol. 313 (2017) 323–331, https://doi.org/10.1016/j.powtec.2017.03.033.
[148] B.J. Chiaramonte de Castro, R. Sartim, V.G. Guerra, M.L. Aguiar, Hybrid air filters: a review of the main equipment configurations and results, Process. Saf. Environ. 144 (2020) 193–207, https://doi.org/10.1016/j.psep.2020.07.025.
[149] K. Chen, Y. Huang, S. Wang, Z. Zhu, T. Lou, H. Cheng, Experimental study on graded capture performance of fine particles with electrostatic-fabric integrated precipitator, Powder Technol. 402 (2022), 117297, https://doi.org/10.1016/j.powtec.2022.117297.
[150] Z. Feng, S.-J. Cao, F. Haghighat, Removal of SARS-CoV-2 using UV+Filter in built environment, Sustain. Cities Soc. 74 (2021), 103226, https://doi.org/10.1016/j.scs.2021.103226.
[151] J.B. Xiang, C.J. Weschler, J.H. Mo, D. Day, J.F. Zhang, Y.P. Zhang, Ozone, electrostatic precipitators, and particle number concentrations: correlations observed in a real office during working hours, Environ. Sci. Technol. 50 (18) (2016) 10236–10244, https://doi.org/10.1021/acs.est.6b03069.
[152] D.B. Day, J. Xiang, J. Mo, M.A. Clyde, C.J. Weschler, F. Li, J. Gong, M. Chung, Y. Zhang, J. Zhang, Combined use of an electrostatic precipitator and a high-efficiency particulate air filter in building ventilation systems: effects on cardiorespiratory health indicators in healthy adults, Indoor Air 28 (3) (2018) 360–372, https://doi.org/10.1111/ina.12447.
[153] S.H. Kim, C. Sioutas, M.C. Chang, Electrostatic enhancement of the collection efficiency of stainless steel fiber filters, Aerosol. Sci. Technol. 32 (3) (2000) 197–213, https://doi.org/10.1080/027868200303731.
[154] W. Jung, J.S. Lee, S. Han, S.H. Ko, T. Kim, Y.H. Kim, An efficient reduced graphene-oxide filter for PM2.5 removal, J. Mater. Chem. 6 (35) (2018) 16975–16982, https://doi.org/10.1039/c8ta04587a.
[155] D.Y. Choi, K.J. Heo, J. Kang, E.J. An, S.-H. Jung, B.U. Lee, H.M. Lee, J.H. Jung, Washable antimicrobial polyester/aluminum air filter with a high capture efficiency and low pressure drop, J. Hazard Mater. 351 (2018) 29–37, https://doi.org/10.1016/j.jhazmat.2018.02.043.
[156] M.-W. Kim, S. An, H. Seok, A.L. Yarin, S.S. Yoon, Transparent metallized microfibers as recyclableelectrostatic air filters with ionization, ACS Appl. Mater. Interfaces 12 (22) (2020) 25266–25275, https://doi.org/10.1021/acsami.0c01697.
[157] K. Noh, J. Lee, C. Kim, S. Yi, J. Hwang, Y. Yoon, Filtration of submicron aerosol particles using a carbon fiber ionizer-assisted electret filter, Aerosol Air Qual. Res. 11 (7) (2011) 811–821, https://doi.org/10.4209/aaqr.2011.05.0060.
[158] Z. Feng, S.-J. Cao, A newly developed electrostatic enhanced pleated air filters towards the improvement of energy and filtration efficiency, Sustain. Cities Soc. 49 (2019), 101569, https://doi.org/10.1016/j.scs.2019.101569.
[159] E. Lachendro, P.J. McKinney, M. Hernandez, Factors affecting bioaerosol inactivation through electrically enhanced germicidal air filters, in: The 11th International Conference on Indoor Air Quality and Climate, Indoor Air, Copenhagen, Denmark, 2008, 2008.
[160] Y. Gu, E. Tian, F. Xia, T. Yu, A. Afshari, J. Mo, A new pin-to-plate corona discharger with clean air protection for particulate matter removal, Energy Built Environ 1 (1) (2020) 87–92, https://doi.org/10.1016/j.enbenv.2019.11.006.
[161] Z. Chen, E. Tian, J. Mo, Removal of gaseous DiBP and DnBP by ionizer-assisted filtration with an external electrostatic field, Environ. Pollut. 267 (2020), 115591, https://doi.org/10.1016/j.envpol.2020.115591.
[162] Y. Gao, E. Tian, Y. Zhang, J. Mo, Utilizing electrostatic effect in fibrous filters for efficient airborne particles removal: principles, fabrication, and material

properties, Appl. Mater. Today 26 (2022), 101369, https://doi.org/10.1016/j.apmt.2022.101369.
[163] C. Kanaoka, S. Hiragi, W. Tanthapanichakoon, Stochastic simulation of the agglomerative deposition process of aerosol particles on an electret fiber, Powder Technol. 118 (1–2) (2001) 97–106, https://doi.org/10.1016/s0032-5910(01)00299-6.
[164] Y. Bian, S. Wang, L. Zhang, C. Chen, Influence of fiber diameter, filter thickness, and packing density on PM2.5 removal efficiency of electrospun nanofiber air filters for indoor applications, Build. Environ. 170 (2020), 106628, https://doi.org/10.1016/j.buildenv.2019.106628.
[165] H. Gao, W. He, Y.-B. Zhao, D.M. Opris, G. Xu, J. Wang, Electret mechanisms and kinetics of electrospun nanofiber membranes and lifetime in filtration applications in comparison with corona-charged membranes, J. Membr. Sci. 600 (2020), 117879, https://doi.org/10.1016/j.memsci.2020.117879.
[166] Y.E. Prawatya, M.B. Neagoe, T. Zeghloul, L. Dascalescu, Surface-electric-potential characteristics of triboand corona-charged polymers: a comparative study, IEEE Trans. Ind. Appl. 53 (3) (2017) 2423–2431, https://doi.org/10.1109/tia.2017.2650145.
[167] R. Zhang, B. Liu, A. Yang, Y. Zhu, C. Liu, G. Zhou, J. Sun, P.-C. Hsu, W. Zhao, D. Lin, Y. Liu, A. Pei, J. Xie, W. Chen, J. Xu, Y. Jin, T. Wu, X. Huang, Y. Cui, In situ investigation on the nanoscale capture and evolution of aerosols on nanofibers, Nano Lett. 18 (2) (2018) 1130–1138, https://doi.org/10.1021/acs.nanolett.7b04673.
[168] A. Peters, H.E. Wichmann, T. Tuch, J. Heinrich, J. Heyder, Respiratory effects are associated with the number of ultrafine particles, Am. J. Respir. Crit. Care Med. 155 (4) (1997) 1376–1383, https://doi.org/10.1164/ajrccm.155.4.9105082.
[169] S. Clifford, M. Mazaheri, F. Salimi, W.N. Ezz, B. Yeganeh, S. Low-Choy, K. Walker, K. Mengersen, G.B. Marks, L. Morawska, Effects of exposure to ambient ultrafine particles on respiratory health and systemic inflammation in children, Environ. Int. 114 (2018) 167–180, https://doi.org/10.1016/j.envint.2018.02.019.
[170] H. Yao, Y. Song, Y. Chen, N. Wu, J. Xu, C. Sun, J. Zhang, T. Weng, Z. Zhang, Z. Wu, L. Cheng, D. Shi, X. Lu, J. Lei, M. Crispin, Y. Shi, L. Li, S. Li, Molecular architecture of the SARS-CoV-2 virus, Cell 183 (3) (2020) 730–738, https://doi.org/10.1016/j.cell.2020.09.018.
[171] X. Zhang, J. Wu, L.M. Smith, X. Li, O. Yancey, A. Franzblau, J.T. Dvonch, C. Xi, R. L. Neitzel, Monitoring SARS-CoV-2 in air and on surfaces and estimating infection risk in buildings and buses on a university campus, J. Expo. Sci. Environ. Epidemiol. (2022), https://doi.org/10.1038/s41370-022-00442-9.
[172] A.J. Jinia, N.B. Sunbul, C.A. Meert, C.A. Miller, S.D. Clarke, K.J. Kearfott, M. M. Matuszak, S.A. Pozzi, Review of sterilization techniques for medical and personal protective equipment contaminated with SARS-CoV-2, IEEE Access 8 (2020) 111347–111354, https://doi.org/10.1109/ACCESS.2020.3002886.
[173] A.K. Cramer, D. Plana, H. Yang, M.M. Carmack, E. Tian, M.S. Sinha, D. Krikorian, D. Turner, J. Mo, J. Li, R. Gupta, H. Manning, F.T. Bourgeois, S.H. Yu, P.K. Sorger, N.R. LeBoeuf, Analysis of SteraMist ionized hydrogen peroxide technology in the sterilization of N95 respirators and other PPE, Sci. Rep. 11 (1) (2021), https://doi.org/10.1038/s41598-021-81365-7, 2051.
[174] D.T. Weaver, B.D. McElvany, V. Gopalakrishnan, K.J. Card, D. Crozier, A. Dhawan, M.N. Dinh, E. Dolson, N. Farrokhian, M. Hitomi, E. Ho, T. Jagdish, E. S. King, J.L. Cadnum, C.J. Donskey, N. Krishnan, G. Kuzmin, J. Li, J. Maltas, J. Mo, J. Pelesko, J.A. Scarborough, G. Sedor, E. Tian, G.C. An, S.A. Diehl, J. G. Scott, UV decontamination of personal protective equipment with idle laboratory biosafety cabinets during the COVID-19 pandemic, PLoS One 16 (7) (2021), e0241734, https://doi.org/10.1371/journal.pone.0241734.
[175] Z. Sun, Y. Yue, W. He, F. Jiang, C.-H. Lin, D.Y.H. Pui, Y. Liang, J. Wang, The antibacterial performance of positively charged and chitosan dipped air filter media, Build. Environ. 180 (2020), 107020, https://doi.org/10.1016/j.buildenv.2020.107020.
[176] J.H. Park, K.Y. Yoon, Y.S. Kim, J.H. Byeon, J. Hwang, Removal of submicron aerosol particles and bioaerosols using carbon fiber ionizer assisted fibrous medium filter media, J. Mech. Sci. Technol. 23 (7) (2009) 1846–1851, https://doi.org/10.1007/s12206-009-0613-z.
[177] M.C. Plopeanu, P.V. Notingher, L.M. Dumitran, B. Tabti, A. Antoniu, L. Dascalescu, Surface potential decay characterization of non-woven electret filter media, IEEE Trans. Dielectr. Electr. Insul. 18 (5) (2011) 1393–1400, https://doi.org/10.1109/tdei.2011.6032807.
[178] E. Tian, Y. Gao, J. Mo, Electrostatically assisted air coarse filtration for energy efficient ambient particles removal: long-term performance in real environment and influencing factors, Build. Environ. 164 (2019), 106348, https://doi.org/10.1016/j.buildenv.2019.106348.
[179] H. Zhang, X. Zhang, P. Wang, R. Chen, G. Gu, S. Hu, R. Tian, Laminated polyacrylonitrile nanofiber membrane codoped with boehmite nanoparticles for efficient electrostatic capture of particulate matters, Nanotechnology 32 (23) (2021), 235601, https://doi.org/10.1088/1361-6528/abeadc.
[180] M.C. Turner, M. Jerrett, C.A. Pope, D. Krewski, S.M. Gapstur, W.R. Diver, B. S. Beckerman, J.D. Marshall, J. Su, D.L. Crouse, R.T. Burnett, Long-term ozone exposure and mortality in a large prospective study, Am. J. Respir. Crit. Care Med. 193 (10) (2016) 1134–1142, https://doi.org/10.1164/rccm.201508-1633OC.
[181] S. Liu, Q. Huang, Y. Wu, Y. Song, W. Dong, M. Chu, D. Yang, X. Zhang, J. Zhang, C. Chen, B. Zhao, H. Shen, X. Guo, F. Deng, Metabolic linkages between indoor negative air ions, particulate matter and cardiorespiratory function: a randomized, double-blind crossover study among children, Environ. Int. 138 (2020), 105663, https://doi.org/10.1016/j.envint.2020.105663.
[182] W. Liu, J. Huang, Y. Lin, C. Cai, Y. Zhao, Y. Teng, J. Mo, L. Xue, L. Liu, W. Xu, X. Guo, Y. Zhang, J. Zhang, Negative ions offset cardiorespiratory benefits of PM2.5 reduction from residential use of negative ion air purifiers, Indoor Air 31 (1) (2021) 220–228, https://doi.org/10.1111/ina.12728.
[183] H. Shen, M. Han, Y. Shen, D. Shuai, Electrospun nanofibrous membranes for controlling airborne viruses: present status, standardization of aerosol filtration tests, and future development, ACS Environ. Au 2 (4) (2022) 290–309, https://doi.org/10.1021/acsenvironau.1c00047.